

Rediagnosis and redescription of *Mosasaurus hoffmannii* (Squamata: Mosasauridae) and an assessment of species assigned to the genus *Mosasaurus*

HALLIE P. STREET*† & MICHAEL W. CALDWELL*‡

*Department of Biological Sciences, University of Alberta, Edmonton, Alberta T6G 2E9, Canada

‡Department of Earth and Atmospheric Sciences, University of Alberta, Edmonton, Alberta T6G 2E9, Canada

(Received 24 August 2015; accepted 4 March 2016; first published online 13 May 2016)

Abstract – The large Late Cretaceous marine reptile *Mosasaurus* has remained poorly defined, in part owing to the unorthodox (by today's nomenclatural standards) manner in which the name was erected. The lack of a diagnosis accompanying the first use of either the genus or species names allowed the genus to become a catchall taxon, and subsequent diagnoses did little to refine the concept of *Mosasaurus*. We herein present emended diagnoses for both *Mosasaurus* and the type species *M. hoffmannii*, based solely on personal examination of the holotype, and a description of the type species based on personal examination of many specimens. *Mosasaurus* exhibits a premaxilla with a short, conical edentulous rostrum, a maxilla with little to no dorsal excavation for the external naris, posteromedial processes of the frontal that deeply invade the parietal, a quadrate taller than long with a short suprastapedial process and the stapedial pit dorsal to the mid-height of the shaft, an angular that is laterally visible for only a short length of the post-dentary unit, a very tall surangular, a humerus with the postglenoid process robust and offset and a distal width greater than the length, and a pubis with an anteriorly projecting tubercle. *M. hoffmannii* is distinguished from other species assignable to the genus by the anteroventral corner formed on the tympanic rim of the quadrate, the asymmetric carinae of the anterior marginal teeth dividing the tooth circumference into short labial and long lingual segments, and the proximal and distal expansion of the femur.

Keywords: anatomy, description, emended diagnosis, Late Cretaceous, mosasaur.

1. Introduction

The first report of the discovery of mosasaur fossils dates to The Netherlands in the 1760s, when an incomplete skull was excavated from upper Maastrichtian chalk quarries of St Pieter's Mountain, Maastricht (Cuvier, 1808). However, this specimen did not garner as much attention as the second larger and much more complete skull (Fig. 1a), which was excavated during the early 1780s from the same underground quarries (Bardet & Jagt, 1996; Bardet, 2012a; Pieters *et al.* 2012), and this is now the holotype of *Mosasaurus hoffmannii* Mantell, 1829, and additionally the namesake of the entire group as established by Gervais (1852).

Awareness of this remarkable fossil animal was so widespread that in November 1794, during the siege of Maastricht, the French revolutionary army seized the specimen when they captured the city (Bardet & Jagt, 1996; Bardet, 2012a; Pieters *et al.* 2012). Around the same time that the skull arrived in Paris (January 1795), a young anatomist, Georges Cuvier, who would go on to write the best-known description of the fossil (Cuvier, 1808), began his appointment at the Museum Nationale d'Histoire Naturelle, Jardin des Plantes, Paris (Bardet & Jagt, 1996; Bardet, 2012a).

The concept of extinction also had not gained widespread acceptance among natural scientists at the time of the discovery of this specimen. Therefore, the morphology of the fossil greatly puzzled contemporary naturalists who struggled to identify the specimen as a member of a group of living animals. J. L. Hoffmann, a surgeon in Maastricht who is said to have paid local quarry workers to inform him when they discovered fossils during their work, considered the remains to be those of a crocodile, but he never finished his study so the first published record of the specimen was by Buc'hoz (1782), who did not attempt to classify the animal as it was unknown to him (Bardet & Jagt, 1996). Four years later, P. Camper (1786) classified the specimen as a large toothed whale based primarily on jaw and tooth morphology, but also considering postcranial features. Van Marum (1790) also considered it to be a whale (or whale type of fish after the classification of Linnaeus still accepted at the time), but based his identification on the presence of pterygoid teeth, which whales do not possess. Faujas de Saint-Fond (1799) reverted to the earlier opinion of classifying the fossil as a crocodile, because he believed the teeth and jaws resembled those of a gavial.

It was not until more than 25 years after the original discovery of the fossil that its broad-scale phylogenetic affinities were recognized. The procoelous vertebrae

†Author for correspondence: hallie.street@gmail.com

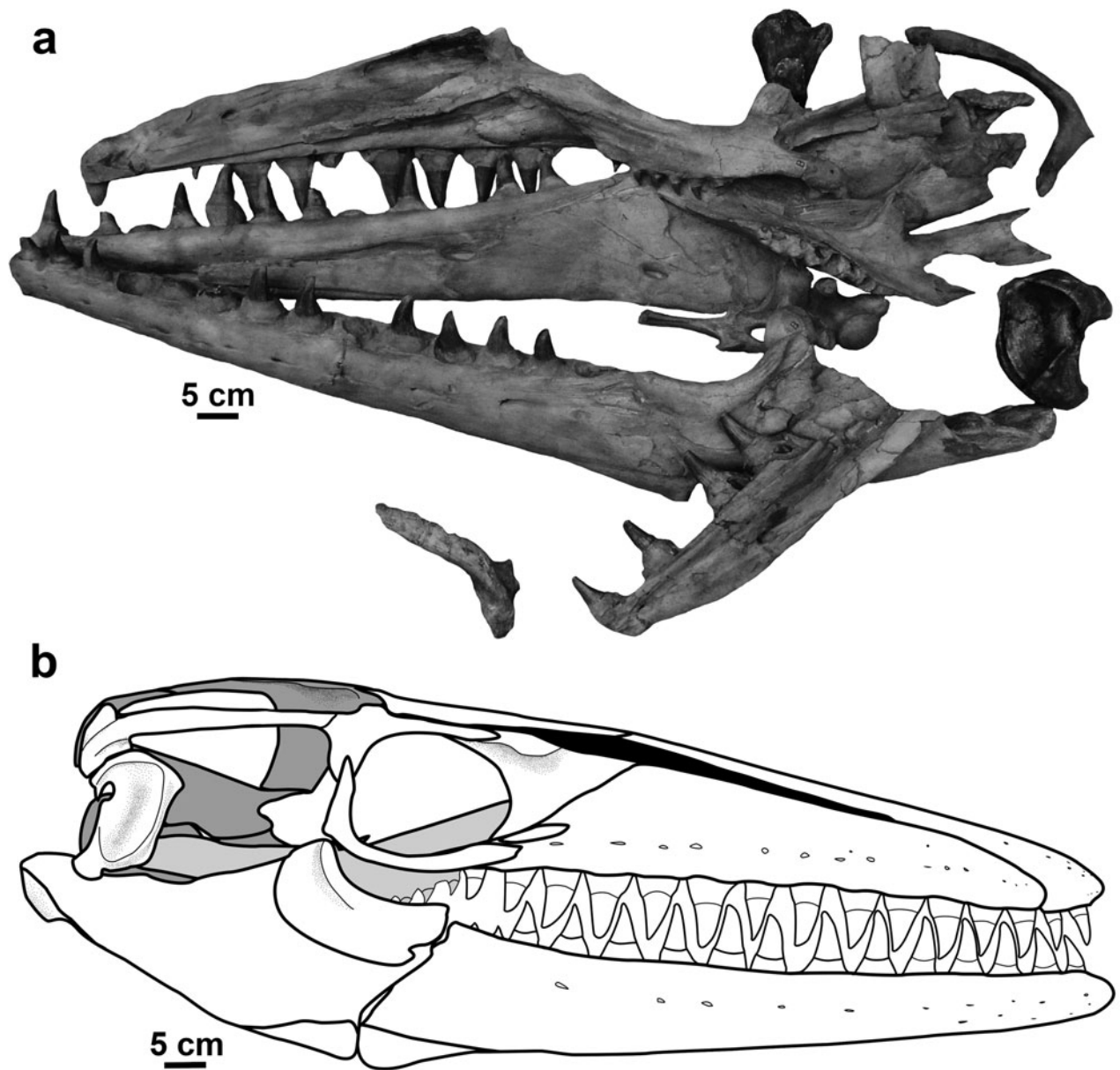


Figure 1. (a) MNHN AC 9648 *Mosasaurus hoffmannii* holotype specimen. (b) Skull reconstruction. Grey shading used to indicate depth within the skull with the light grey pterygoid lying between the white external skull elements and the dark grey midline braincase elements; black indicates narial opening. Premaxilla, maxilla, dentary, splenial, angular, surangular, coronoid, articular, pterygoid based on IRSNB R 26; prefrontal, frontal, postorbitofrontal, parietal based on NHMUK 42929; jugal, squamosal, quadrate based on NMHN AC 9648; basisphenoid, basioccipital, paroccipital bar, based on YPM 430. Some interpretation required for articulation between paroccipital bar, supratemporal, parietal, basisphenoid. Scale bar absolute for jaw elements, the rest of the skeletal elements were scaled to fit. Note: letters visible on the fossil have been painted on the specimen and bear no association with the labelling system of this study. Scale bars equal 5 cm.

and, even more significantly, the lower jaw comprised of multiple bones, were used by A. Camper (1800) to conclude that the animal was a type of lizard and not a whale. Cuvier (1808) wrote the most extensive description of the specimen of the time and also considered 'le grand animal fossil des carrières de Maestricht' to resemble monitor lizards based on dental characters such as mode of tooth replacement. Also, like Camper (1800), Cuvier (1808) considered the fossil to

represent a marine organism that swam via lateral undulation of the caudal region and that it was an animal unlike any alive.

Once the uncertainty surrounding the classification of 'le grand animal' was clarified by the studies of Camper (1800, 1812) and Cuvier (1808), who established its identity as an extinct marine lizard, a new era of confusion began because, despite the common use of binomials for species names, Cuvier did not erect

a name to accompany his description. In 1816 Sömmerring created the name *Lacerta gigantea*, for what is now recognized to be a Jurassic crocodylian, because he believed it to be a juvenile of the Maastricht specimen (Bardet & Jagt, 1996; Young & de Andrade, 2009). The generic name *Mosasaurus* (but no associated specific epithet) was unconventionally erected when Parkinson (1822) published a conversation with Conybeare who had suggested to him the naming of ‘le grand animal’ after the Maas/Mosa (Dutch/Latin) River where the specimen was found, until Cuvier decided on a more permanent name. Cuvier never proposed an alternative name and eventually adopted *Mosasaurus* into his own work (Cuvier, 1829).

The specimen remained without a specific epithet until 1829 when two different names were proposed by two different authors (Holl, 1829; Mantell, 1829), though, as pointed out by Bardet & Jagt (1996), each specific epithet has its own taxonomic issues. *Mosasaurus belgicus* Holl, 1829 is a misnomer because the fossil actually originates from The Netherlands. While describing the first mosasaur fossils from England, Mantell (1829) erected the name ‘*Mososaurus*’ *hoffmannii*. Despite Mantell’s intention to assign the British specimens to the Maastricht taxon, he never formally did so. In this sense, despite the contradictory common usage, the binomial *M. hoffmannii* should technically be associated with the vertebrae from England, not the skull described by Cuvier (Bardet & Jagt, 1996). In 1832 Meyer attempted to synonymize *M. hoffmannii* and *Lacerta gigantea* with his new species *Mosasaurus camperi* and ignored *M. belgicus* (Bardet & Jagt, 1996). Charlesworth (1846) suggested a solution to the issues surrounding Mantell’s *Mosasaurus hoffmannii*: a new species, *Mosasaurus stenodon* Charlesworth, 1846, was erected for the British material in order to maintain the name *M. hoffmannii* for ‘le grand animal’ (Camp, 1942; Bardet & Jagt, 1996). Despite Charlesworth’s suggestion, *camperi*, *hoffmannii* and *giganteus* were all used by various authors to describe the Maastricht specimen until Camp (1942) determined that *M. hoffmannii* was the most acceptable name (Bardet & Jagt, 1996).

Following Camp’s (1942) opinion on the appropriate specific epithet for the Paris specimen, Russell (1967) emended the generic diagnosis of *Mosasaurus* based solely on North American species and specimens without viewing the European species or the holotype. Lingham-Soliar (1995) published an emended diagnosis of *M. hoffmannii*, but that diagnosis remains uninformative and based partially on referred specimens, not solely on the type specimen. Mantell (1829) originally spelled the specific epithet with two ‘ii’s, but subsequent authors dropped the second ‘i’, a convention that has largely been followed to this day. This issue was addressed by Konishi, Newbrey & Caldwell (2014) who determined that the use of two ‘ii’s, besides being the original spelling and therefore inherently valid, is not incorrect. Therefore, it was determined

that the species represented by MNHN AC 9648 should be called *Mosasaurus hoffmannii*.

Mosasaur fossils have been known for approximately 250 years, fossils from around the world have been referred to the type species (Bardet, 2012b; Bardet *et al.* 2014) and yet the taxonomy of the type genus and species are incredibly unstable owing to the improper way in which the names were erected. Stabilizing the concept of *Mosasaurus* in order to ensure the longevity and informative value of the genus is thus of great importance. Previous attempts to define *Mosasaurus* were limited by lack either of context (Camper, 1800; Cuvier, 1808), nomenclatural guidelines (Conybeare *in* Parkinson, 1822; Mantell, 1829) or access to significant fossils (Russell, 1967).

Cuvier (1808) like A. Camper before him (1800) described the skull of the holotype specimen, with particular attention paid to the jaws and teeth. While both conducted detailed comparative studies and recognized the similarities between the fossil and monitor lizards and iguanas, as opposed to the affinities to crocodiles or whales espoused by previous authors (Camper, 1786; Van Marum, 1790; Faujas de Saint-Fond, 1799), neither went further with their classification or attempted to assign a name to the specimen. Their collective work established what the fossil looked like, a better idea of how to classify it, but most importantly what type of animal the fossil was not.

As Camp (1942) noted, and the above summary attests, the palaeontological literature abounds with descriptions, diagnoses, emended diagnoses and various opinions as to the identity and relationships of the ‘grand animal fossil des carrières de Maestricht’ (Hoffmann; Buc’Hoz, 1782; Camper, 1786; Van Marum, 1790; Faujas de Saint-Fond, 1799; Camper, 1800; Cuvier, 1808; Parkinson, 1822; Holl, 1829; Mantell, 1829; Meyer, 1832). Despite consensus on the appropriate name for the species since Camp (1942), and an emended diagnosis by Lingham-Soliar (1995), the taxonomy of the genus that *Mosasaurus hoffmannii* is considered to typify remains unclear. The relationships of the species within the genus, and the relationships between *Mosasaurus* and related genera cannot be accurately determined without a clearer understanding of what morphological features define the type species, and which of those features are shared by all species in the genus. A new reconstruction of the skull in lateral view has been generated based on photographs of the skull elements from various fossils across Europe and the United States (Fig. 1b). This study aims to emend the existing diagnoses for *Mosasaurus* and the type species *Mosasaurus hoffmannii* (the latter based solely on the holotype specimen) and to describe *M. hoffmannii*, based on observations of multiple specimens, to serve as the basis for a more extensive generic revision and phylogenetic analysis of various species of *Mosasaurus* and relationships with the Mosasaurinae.

Institutional abbreviations. AL – Alabama Museum of Natural History, Tuscaloosa, United States;

AMNH – American Museum of Natural History, New York, United States; CM – Canterbury Museum, Christchurch, New Zealand; IRSNB – Institut royal des Sciences naturelles de Belgique, Brussels, Belgium; MNHN – Muséum national d'Histoire naturelle, Paris, France; NHMM – Natuurhistorisch Museum Maastricht, Maastricht, The Netherlands; NHMUK – Natural History Museum, London, United Kingdom; NJSM – New Jersey State Museum, Trenton, United States; TSMHN – Teylers Strichtina Museum, Haarlem, The Netherlands; USNM – United States National Museum, Washington, DC, United States; YPM – Yale Peabody Museum, New Haven, United States.

2. Systematic palaeontology

Class REPTILIA Linnaeus, 1758

Order SQUAMATA Opperl, 1811

Family MOSASAURIDAE Gervais, 1852

Subfamily MOSASAURINAE Gervais, 1852

Genus *Mosasaurus* Conybeare, 1822

1822 *Mosasaurus* Conybeare in Parkinson, p. 198.

1839a *Batrachiosaurus* Harlan, p. 24.

1839b *Batrachotherium* Harlan, p. 89.

1849 *Macrosaurus* Owen, p. 382.

1856 *Drepanodon* Leidy, p. 255.

1861 *Lesticodus* Leidy, p. 10.

1865 *Baseodon* Leidy, p. 69.

1868 *Nectoportheus* Cope, p. 181.

1882 *Pterycollosaurus* Dollo, p. 61.

Type species. *Mosasaurus hoffmannii* Mantell, 1829

Emended generic diagnosis. Premaxilla with short, conical edentulous rostrum; maxilla with little to no excavation for external naris; jugal with bowed anterior ramus and reduced but distinct posteroventral process; prefrontal and postorbitofrontal meeting ventral to frontal thereby excluding frontal from margin of orbit; posteromedial processes of frontal deeply invading parietal to embrace parietal foramen; pterygoid tooth row straight; quadrate taller than long with stapedial notch located dorsal to midpoint of shaft; short suprastapedial process, infrastapedial process reduced to bump on posteromedial surface of shaft; stapedial pit oval, oriented obliquely to vertical axis of shaft; quadrate tympanic rim grooved with distinct anterodorsal corner; dentary with short, round edentulous projection; angular decreasing rapidly in height, laterally visible only short length of post-dentary unit; coronoid with tall dorsal process and posterior margin posteriorly curved in lateral view; surangular tall with steeply ascending coronoid buttress that can exhibit dorsal excavations or prominences; retroarticular rotated laterally towards horizontal; marginal teeth faceted labially, bicarinate; cervical centra round; caudal vertebrae with fused chevrons; scapula and coracoid subequal in size; scapula longer posteriorly than anteriorly;

humerus postglenoid process robust and offset; distal length greater than height radial facet straight, ulnar facet convex; pubis with anteriorly projecting tubercle on proximal shaft.

Occurrence. Upper Cretaceous (Campanian and Maastrichtian) formations of Angola, Belgium, Brazil, Bulgaria, Canada, Denmark, Germany, Italy, Japan, Jordan, Morocco, New Zealand, Niger, The Netherlands, Poland, the Russian Federation, South Africa, Spain, Syria, Turkey and the United States.

Mosasaurus hoffmannii Mantell, 1829

(Figs 1–26)

1829 *Mosasaurus hoffmannii* Mantell, p. 207.

1816 *Lacerta gigantea* Sömmering, p. 54.

1829 *Mosasaurus belgicus* Holl, p. 84.

1832 *Mosasaurus camperi* Meyer, pp. 113–14.

1840 *Mosasaurus hoffmanni* Mantell; Owen, p. 261.

1869 *Mosasaurus maximus* Cope, p. 262.

1870 *Mosasaurus giganteus* (Sömmering); Cope, p. 189.

1879 *Mosasaurus camperi* Meyer; Ubaghs, pp. 240–5, pls 1, 2.

1889 *Mosasaurus camperi* Meyer; Dollo, pp. 277–9, pl. 9, fig. 1; pl. 10, figs 12, 13.

1924 *Mosasaurus giganteus* (Sömmering); Dollo, p. 172.

1942 *Mosasaurus hoffmanni* Mantell; Camp, pp. 45–6.

1959 *Mosasaurus hoffmanni* Mantell; Persson, p. 461.

1967 *Mosasaurus hoffmanni* Mantell; Russell, pp. 8, 122, 131–2, 140, 210.

1967 *Mosasaurus maximus* Cope; Russell, pp. 139–40, figs 8, 24a, 80.

1983 *Mosasaurus hoffmanni* Mantell; Meijer, pp. 269–71, fig. 3.

1989 *Mosasaurus hoffmanni* Mantell; Lingham-Soliar & Nolf, pp. 156, 158, 174, figs 52, 175.

1991 *Mosasaurus hoffmanni* Mantell; Lingham-Soliar, p. 665.

1995 *Mosasaurus hoffmanni* Mantell; Lingham-Soliar, pp. 158, 161, figs 1, 3, 5, 6, 9, 12, 14, 16.

1997 *Mosasaurus maximus* Cope; Bell, pp. 297–308, 310–18, 320, 321, 329–32.

1998 *Mosasaurus hoffmanni* Mantell; Kuypers *et al.*, p. 25, fig. 9, pl. 1, figs 1–13, pl. 3, figs 3–10, pl. 9, figs 1–12.

1999 *Mosasaurus hoffmanni* Mantell; Mulder, pp. 283–9, figs 1–14, 16.

2014 *Mosasaurus hoffmannii* Mantell; Konishi, Newbrey & Caldwell, p. 803.

Emended species diagnosis. Quadrate tympanic rim with additional anteroventral corner; maxillary tooth count = 13; dentary tooth count = 14; pterygoid tooth

count = 8; marginal teeth carinae asymmetric anteriorly with lingual circumference greater than labial; cervical vertebra transverse processes elongate with little ventral buttressing; femur greatly expanded medially and distally with articular surfaces nearly perpendicular; internal trochanter robust and offset.

Type. MNHN AC 9648.

Referred material. AL PV 990.003; AMNH 1385; AMNH 1389; AMNH 1386; AMNH 1391; AMNH 1392; AMNH 1393; AMNH 1397; AMNH 1398; AMNH 1404; AMNH 1406; AMNH 1407; AMNH 1461; AMNH 2533; AMNH 4912; AMNH 5149; AMNH 14815; IRSNB R 303; IRSNB R.26; NHMM 000886; NHMM 001450; NHMM 001469-1; NHMM 002457; NHMM 006696; NHMM 006698; NHMM 1989107; NHMM 199348-1; NHMM199348-2; NHMM St9008G; NHMUK 42929; NJSM 11052; NJSM GP11053; IRSNB R 26; IRSNB R 25; IRSNB R 24; IRSNB Vert-00-256; IRSNB R 300; IRSNB R 301; IRSNB R 299; IRSNB R 302; TSMHN 871; TSMHN 5214; TSMHN 7424; TSMHN 11201; TSMHN 11208; TSMHN 11214; TSMHN 11241; TSMHN 11242; TSMHN 11245; TSMHN 11376; TSMHN 112142; USNM 8436; USNM 10540; USNM 391916; USNM 418464; USNM 437647; Y YPM 305; YPM 307; PM 311; YPM 414; YPM 430; YPM 470; YPM 508; YPM 509; YPM 510; YPM 690; YPM 773; YPM 1504.

Occurrence. Bentiaba; Namibe, Angola; Upper Cretaceous Maastrichtian. Craie de Ciply; Belgium; Upper Cretaceous Maastrichtian. Kajlâka Formation; Pleven, Bulgaria; Upper Cretaceous Maastrichtian. Danish White Chalk Formation; Denmark; Upper Cretaceous Maastrichtian. Scaglia Rosa Formation; Italy; Upper Cretaceous Maastrichtian. Muwaddar Chalk Marl Formation; Jordan; Upper Cretaceous Maastrichtian. Nekum Chalk; The Netherlands; Upper Cretaceous Maastrichtian (Kanne Horizon). Greensand Formation, Opoka Formation; Poland; Upper Cretaceous Maastrichtian. Davutlar Formation; Devrekani, Turkey; Upper Cretaceous Maastrichtian. Penza, Russian Federation; Upper Cretaceous Maastrichtian. Ripley Formation, Prairie Bluff Chalk; Alabama, United States; Severn Formation; Maryland, United States; Owl Creek Formation; Missouri, United States; Navesink Formation; New Jersey, United States; Coon Creek Tongue Member, Ripley Formation; Tennessee, United States; Navarro Formation; Texas, United States; Upper Cretaceous Maastrichtian.

3. Description

3.a. Cranial skeleton

3.a.1. Premaxilla

The premaxilla (Fig. 2) of NHMM 006696 exhibits a short, bluntly conical edentulous rostrum anterior to the first pair of premaxillary teeth. The lateral sur-

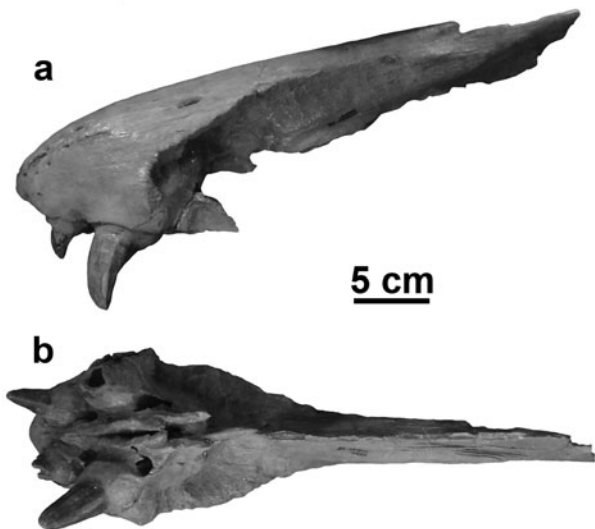


Figure 2. Premaxilla of NHMM 006696 in (a) left lateral view and (b) ventral view. Scale bar equals 5 cm.

faces of the anterior portion of the rostrum are perforated by irregular clusters of foramina (Fig. 2a). There are also larger single or paired foramina posterodorsal to the posterior premaxillary teeth. The profile of the premaxilla slopes dorsally, diverging from the plane formed by the dental margin. Of the four premaxillary teeth, the anterior pair is more gracile than the posterior pair. The premaxilla is widest directly posterior to the second tooth position, behind which the element tapers to form the internarial bar. In cross-section, the internarial bar is T-shaped, being broader dorsally and thinning to a blade-like ridge ventrally. A pair of compressed, posteriorly projecting flanges extend from the tooth-bearing portion of the premaxilla. The premaxilla of IRSNB R 26 is more complete posteriorly, and at the posterior termination of the internarial bar for that specimen the dorsal surface dilates slightly and the ventral vertical ridge bears longitudinal grooves on each lateral surface.

Ventrally (Fig. 2b), between the pairs of premaxillary teeth, there is a pair of ridges, which form a sulcus or vacuity between them along the midline. Anteriorly, this structure tapers to a point between the first pair of teeth and is separated by a groove from the roots of these teeth. Posterior to the second pair of premaxillary teeth, the ridges bifurcate further to form a pair of flanges that articulate laterally and posteriorly with the maxillae and medially with the vomers. The ventral surface of the narrowing dorsal portion of the premaxilla forms broad thin articular facets that articulate with the maxillae.

The logarithmic form of the suture trace between the premaxilla and the maxilla is typically 'mosasaurian' (Fig. 2a). However, this suture is not necessarily a smooth curve. In some cases, the vertical rise of the suture can be convex anteriorly, excavating deeper into the premaxilla, or slightly concave dorsally, excavating into the maxilla before continuing posteriorly.

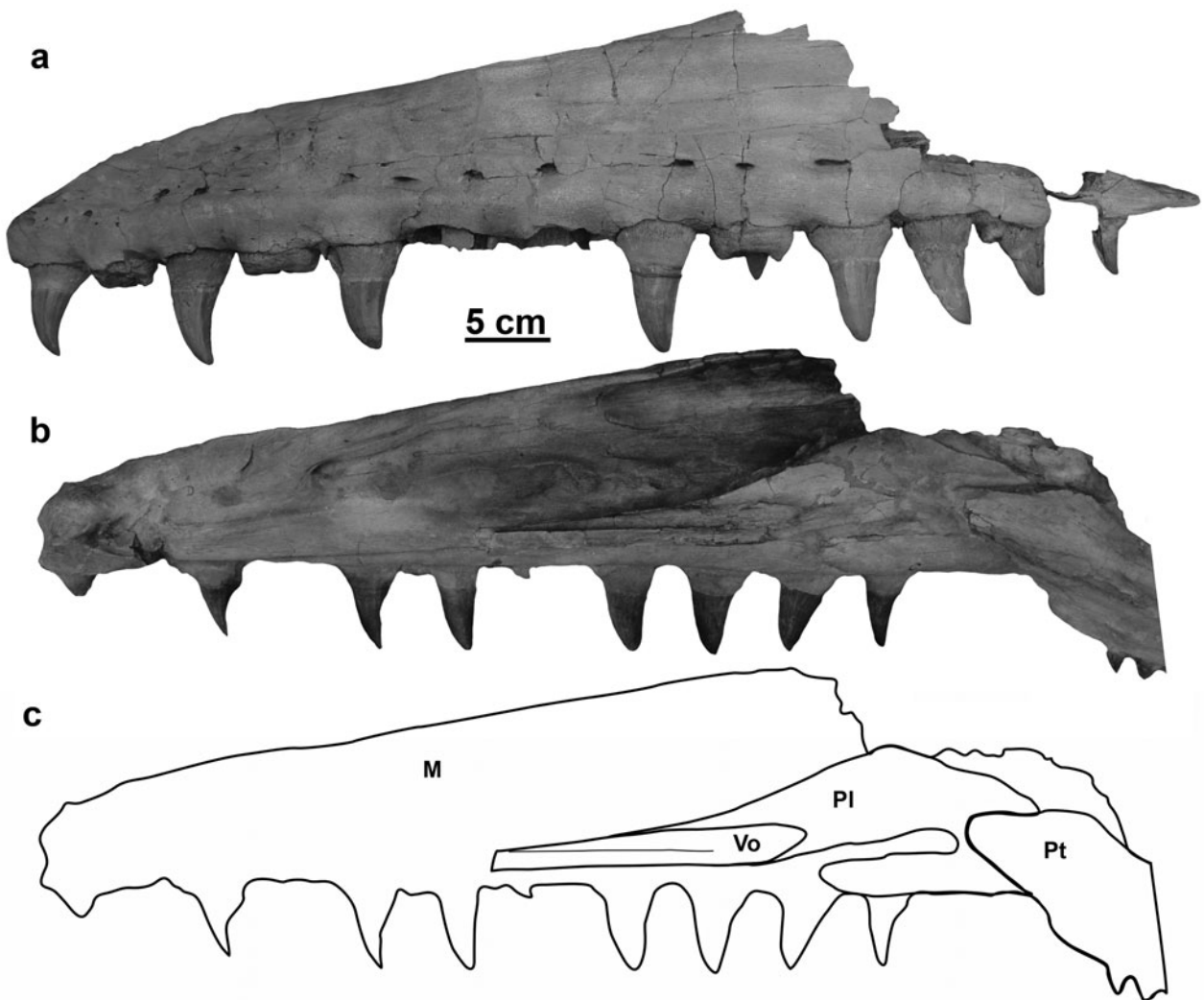


Figure 3. Maxillae. (a) IRSNB R 26 right lateral view (reflected). (b) MNHN AC 9648 right medial view and (c) the same outlined to highlight the palatine and vomer. Abbreviations: M – maxilla; Pl – palatine; Pt – pterygoid; Vo – vomer. Note: letters visible on the fossil have been painted on the specimen and bear no association with the labelling system of this study. Scale bar equals 5 cm.

3.a.2. Maxilla

The lateral surface (Fig. 3a) of the maxilla is perforated by a series of foramina dorsal to the tooth row. The maxilla of MNHN AC 9648 (Fig. 3b) is blunt anteriorly, where the maxillary/premaxillary suture ascends steeply, nearly vertically, from the tooth margin. This morphology differs in IRSNB R 26, and additionally in NHMM 006696, where the maxilla is short in height anteriorly, and the maxillary/premaxillary suture ascends at approximately 35° (Fig. 3a). After the suture turns posteriorly, the dorsal margin of the maxilla rises at a shallow angle until the border is even with the posterior margin of the third maxillary tooth (Fig. 3b). The dorsal margin and tooth row are each straight and the two diverge only slightly from each other, with the maxilla increasing only slightly in height posteriorly, until the level of the eleventh tooth, at which point the height of the element decreases rapidly to form the narrow posterior process of the maxilla. *Mosasaurus hoffmannii* typifies the unique dorsal profile of the maxilla

seen in this genus. In most mosasaurs, the border of the maxilla is concave dorsally; this concavity is the excavation forming the lateral edge of the external naris. In this species, there is little to no concavity for the naris; therefore, the maxilla is straight to gently convex dorsally. Medially, there is an oval-shaped foramina in the dorsal half of the bone between the fourth and fifth teeth, and the dorsal margin of the maxilla bears a sulcus along the border of the external naris. The maxilla bears 13 teeth. These marginal teeth are relatively consistent in size but are smallest posteriorly and largest at the middle of the tooth row, as is typical across Mosasauridae.

3.a.3. Frontal

NHMUK 42929 is a partial skull roof comprised of the frontal, both prefrontals, the left postorbitofrontal and the anterior portion of the parietal. None of the elements are complete, but the fragmentary nature of

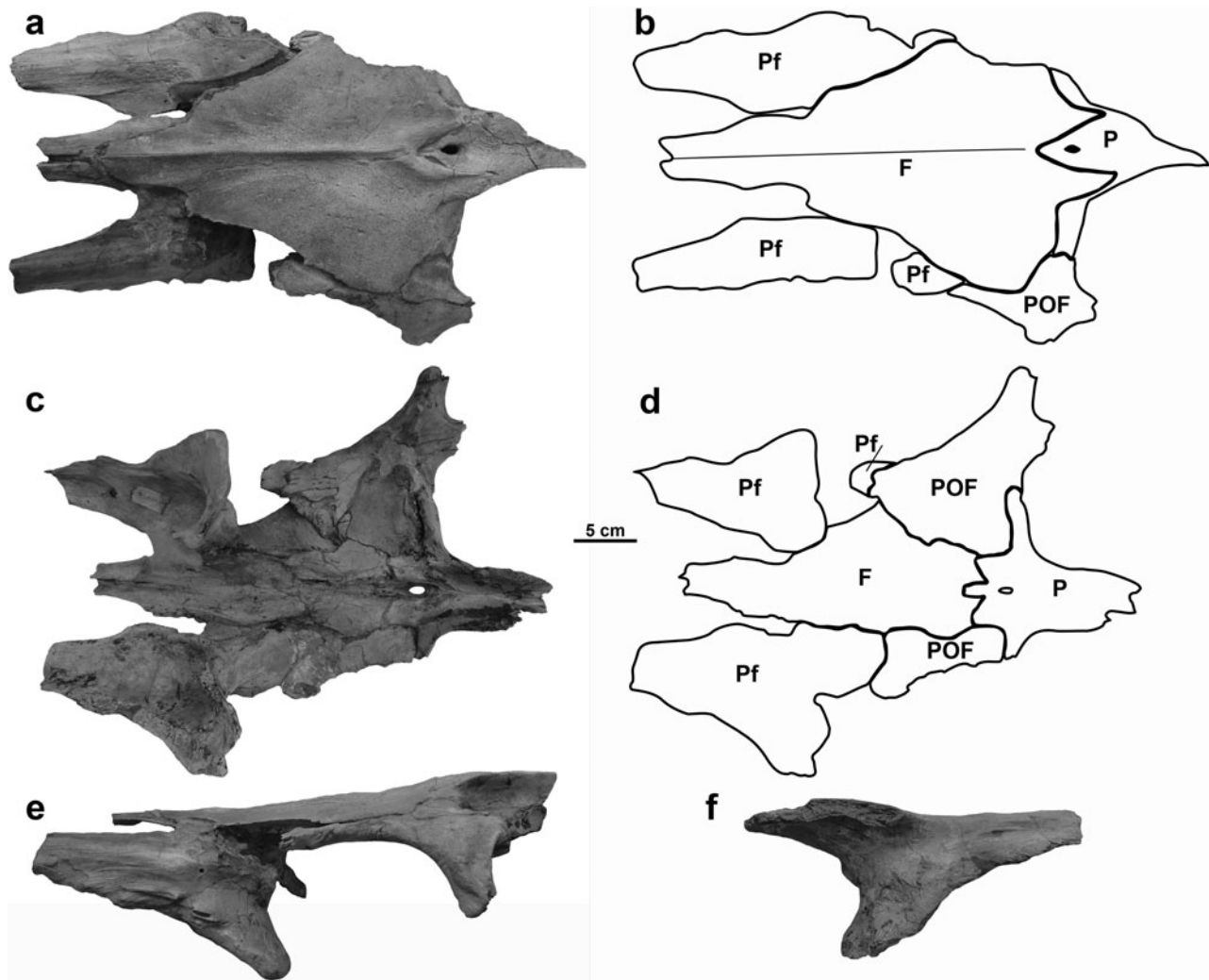


Figure 4. Skull roof of NHMUK 42929 in (a) dorsal view, (b) dorsal view labelled, (c) ventral view, (d) ventral view labelled, (e) left lateral view, and (f) prefrontal right lateral view. Abbreviations: F – frontal; P – parietal; Pf – prefrontal; POF – postorbitofrontal. Scale bar equals 5 cm.

the specimen actually allows for observation of the sutures between these elements, particularly in ventral view.

On the dorsal surface of the frontal, and running the full length of the bone, there is a steep-sided sagittal ridge (Fig. 4a). The anterior termination of the frontal, where it articulates with the premaxilla, is not completely preserved. The anterior-most preserved portion of the frontal forms a narrow, straight-sided neck that extends between the nares and contributes to the internarial bar. The dorsal midline of this anterior neck is marked by a sharp groove, which likely would have accepted a tongue from the premaxilla. The lateral borders of the neck diverge slightly posteriorly and form a first, smaller, set of distinct expansions along the margins of the frontal. Posterior to these expansions, which dictate the posterior termination of the external nares, a thin flange of bone descends ventrolaterally, forming a facet to accept a thin medial wing from the prefrontal. Posterior to the external nares, the lateral borders of the frontal are gently medially concave be-

fore flaring sharply laterally, forming the second, more prominent set of expanded shelves and nearly doubling the width of the bone. Posterior to this second expansion, the lateral borders of the frontal diverge posterolaterally, giving the frontal its overall triangular outline. The edges of the frontal are slightly anterolaterally concave dorsal to the orbits, but the posterolateral corners of the element are rounded. Postero-medially, the dorsal ridge bifurcates and contributes a raised medial border to a pair of posteromedial prongs that overlap the parietal and broadly embrace the parietal foramen. These asymmetrical prongs are thickest medially and thin out posteriorly and laterally as they approach the edge of the parietal table. A shallow depression follows the median ridge from the prongs to the internarial bar and is lateral to the divergence of the prongs.

Ventrally, the frontal supports the medially thickened frontal boss and broad lateral fossae for the articulation of the prefrontals and postorbitofrontals (Fig. 4b–d). As broad as the frontal is, if all the surrounding bones

were in articulation, only a narrow portion of the element would be seen in ventral view. The lateral edges of the frontal boss are shallowly sinusoidal, and diverge only slightly posteriorly. Similar to the dorsal surface, the ventral surface of the anterior neck of the frontal is bisected by a narrow groove to accept a prong from the premaxilla. The ventral groove is longer, extending posteriorly past the point of the first frontal expansion, and is bounded by a ridge on each side. The internarial bar of the premaxilla would have overlapped the anterior-most portion in the frontal tip in 'pinch-like' articulation. The anterolateral portion of the frontal, from the posterior end of the external nares to about the midpoint of the element, is occupied by the facet for the prefrontal. The anteromedial edge of the postorbitofrontal is sandwiched between the frontal ala and the rounded posterior termination of the prefrontal, and medial expansion of the prefrontal and postorbitofrontal constricts the frontal boss at this point. This overlap of the prefrontal and postorbitofrontal excludes the frontal from contributing to the orbit. The postorbitofrontal occupies the broad posterolateral portion of the frontal ala (about two-thirds of the lateral width). These ventral facets of the frontal are smooth to faintly ridged/striated for the articulations with the surrounding bones. Posteriorly, the parietal underlies the frontal with a median process extending anteriorly from the parietal foramen and the lateral wings of the parietal, which in turn are underlain by the posteromedial corners of the postorbitofrontals.

3.a.4. Prefrontal

The prefrontal is a three-dimensionally complex bone that partially encloses the external naris anterodorsomedially (Fig. 4a), the internal naris anteroventromedially (Fig. 4c) and the orbit posteroventrolaterally (Fig. 4e, f). The exposed dorsal surface of the prefrontal is convex around its anteroposterior axis (Fig. 4a). The anteromedial margin of the prefrontal forms the posterolateral edge of the external naris. While the dorsal surface of the prefrontal is seen to narrow anteriorly, the rostral end is incomplete so the extent of the articulation with the maxilla is not known. Posteromedially, the prefrontal underlies the lateral margin of the frontal. The supraorbital process is also unknown, but the broken bone surface indicates that such a process was present and had a concave ventral surface (Fig. 4f).

In *Mosasaurus hoffmannii*, the lateral surface of the prefrontal is more robust than the 'thin lateral lamina' described by Russell (1967, p. 21) (Fig. 4e, f). The descending wing greatly increases in height posteriorly giving the prefrontal a steep anteroventral border for the articulation to the posterodorsal margin of the maxilla. Dorsal to the middle of this articular margin, the left prefrontal bears a notable rugosity, but whether this reflects a pathological condition of the left prefrontal or poor preservation of the right is un-

clear. The lateral wing curves medially to form the posteriorly concave anterior wall of the orbit, while the ventral-most extent of the lateral wing curves posteriorly.

Internally, the prefrontal is no less complex (Fig. 4c, d). The posterodorsal border is U-shaped and underlies the anterior-most extent of the postorbitofrontal. The dorsomedial border articulates with the frontal boss, and the lateral side forms the orbit. Posteroventrally, the prefrontal bears a hook- or J-shaped facet for articulation with the palatine ventrally. This facet is greatly expanded posterolaterally into a broad, triangular articular surface. This portion of the bone is deeply excavated and with the presumed concavity of the palatine, would form a large internal narial capsule.

3.a.5. Postorbitofrontal

The postorbitofrontal is largely incomplete, but most of its processes are sufficiently intact to merit description (Fig. 4). Of the four divergent processes of the postorbitofrontal, the posterior process to the squamosal is the least complete. The dorsal exposure of the postorbitofrontal embraces the frontal ala (Fig. 4a). A short, broad process extends medially, along the posterolateral edge of the frontal to contact the anterolateral wing of the parietal and contributes to about one-third of the anterior border of the supratemporal fenestra. The anterior process of the postorbitofrontal extends anteriorly along the lateral edge of the frontal, forming the posterodorsal border of the orbit (Fig. 4e). Anteriorly, the postorbitofrontal contacts the prefrontal in an anteroventrally oblique suture, thereby excluding the frontal from contributing to the orbit (Fig. 4b).

The ventral surface of the postorbitofrontal describes a broad curve, which forms the posterodorsal border of the orbit (Fig. 4e). The descending arc of this border is formed by the well-preserved ventral ramus of the postorbitofrontal. The ventral ramus is shorter than the anterior process and broader than the medial process. Laterally, this ramus bears two depressions. The first is a facet at the anterolateral termination of the process where the jugal would articulate. The posterior edge of the ventral ramus is pinched into a thinner, longer depression connecting the ventral process with the posterior process.

The posterior process is largely incomplete, with just the base remaining. In dorsal view, this process narrows considerably from the broad body of the postorbitofrontal between the medial and ventral processes (Fig. 4a). Laterally, this process would have been taller than the anterior process, bearing a sharp keel that would insert into the corresponding groove on the squamosal.

The postorbitofrontal is much more extensive internally (Fig. 4c, d). A large wing of bone extends medially from the anterior process and joins the anterior and

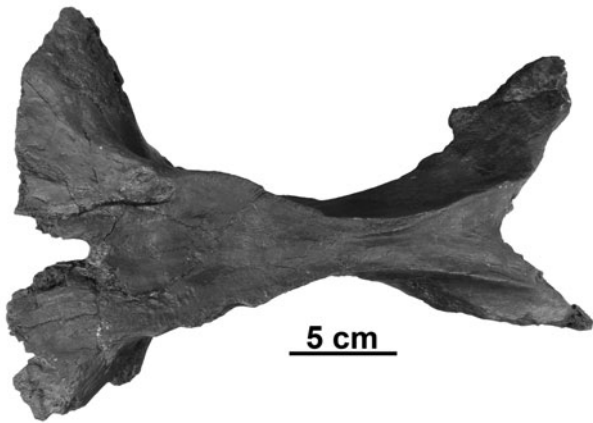


Figure 5. Parietal NJSM 11052 in dorsal view. Scale bar equals 5 cm.

medial processes. Anteromedially, this wing of the postorbitofrontal is sandwiched between the frontal dorsally and the posterior edge of the prefrontal ventrally. The medial border of the postorbitofrontal follows the undulating margin of the frontal boss, and the wing is broadest posteriorly. The sutures between the posterior border of the postorbitofrontal wing and the parietal forms a step-like pattern: the border between the postorbitofrontal and the parietal is oriented anteroposteriorly medially where the parietal contributes to the posterior end of the frontal boss; it then turns laterally at approximately a right angle, where the lateral wing of the parietal bounds the posteromedial edge of the postorbitofrontal. And finally, the border curves again at a slightly obtuse angle, where the postorbitofrontal bounds the anteroposteriorly short lateral termination of the parietal.

3.a.6. Parietal

Only the anteromedial portion of the parietal of NHMUK 42929 is preserved, but it does provide a good deal of information about the sutures with the frontal and the postorbitofrontals. Additionally, a partial parietal comprises part of a disarticulated skull (NJSM 11052) originally described as *Mosasaurus 'maximus'* Cope, 1869 (Figs 4a, 5). Dorsally, the parietal table narrows posterior to the termination of the prongs from the frontal (Fig. 4a). This constriction occurs immediately posterior to the prongs in NHMUK 42929, but in NJSM 11052 the parietal table continues to be broad for a distance approximately equal to the length of the frontal prongs posterior to the parietal foramen. The small, elliptical parietal foramen occupies the parietal table between the frontal prongs. Anterior to the foramen, the parietal table terminates in a point and is fluted where it plunges under the frontal. Posterior to the constriction, the borders of the parietal table extend parallel to each other before flaring laterally to termin-

ate on the posterior edge of each suspensory ramus of the parietal, but the posterior width of the parietal table is less than the anterior width. The edges of the parietal table are sharp and, for the portion of the element anterior to the constriction, form shelves that overhang the descending processes of the parietal. Anteriorly, lateral to the prongs from the frontal, two arms of the parietal follow the posterior margin of the frontal and terminate in a suture with the postorbitofrontals. Posteriorly, the two suspensory rami are obliquely dorsoventrally compressed and extend relatively horizontally from the plane of the parietal table. The suspensory rami diverge at an obtuse angle, only slightly larger than 90° , and would continue ventrolaterally to contact the supratemporals, but they are incomplete in NJSM 11052.

Ventrally the parietal is longitudinally concave (Fig. 4c). Anteriorly, the parietal widens to form lateral arms on either side of the parietal foramen, which is bevelled out into a longer groove. The margins of this groove form a sharp crest that extends anteriorly and posteriorly along the midline. The anteroventral border of the parietal is complex. Anteromedially, the parietal forms a squared-off process anterior to the parietal foramen, but the border forms an acute angle and extends away from the midline anterolaterally from the crest around the parietal foramen, which is then truncated by the posteromedial corner of the postorbitofrontal. The longitudinal concavity recognized in NHMUK 42929 continues the length of the parietal table of NJSM 11052 between the two descending processes of the parietal. The mediolateral distance between these two processes increases ventrally, but the processes converge posteriorly. The poor preservation of the ventrum of the parietal of NJSM 11052 prevents additional observations, such as the height of the descending processes.

3.a.7. Jugal

There is a possibility, as highlighted by Bardet (2012a), that the femur, along with the left quadrate and squamosal and right jugal, now associated with MNHN AC 9648 does not come from the same individual as the rest of the skull. These elements were not described by Cuvier (1808) and are loose, rather than being embedded in the block. Additionally, they are a different colour than the rest of the specimen, but this appears to be due to a coating of varnish or glue. The quadrate agrees in size with the partial right quadrate embedded in the block, so these elements will be treated as belonging to the same specimen.

The jugal of MNHN AC 9648 bears a short dorsal ramus that broadens ventrally where it contributes to the reduced posteroventral process (Fig. 6). This process forms a sharp point posteriorly, and bears a shallow sulcus ventrolaterally (Fig. 6a). The anterior ramus of the jugal is bowed so that the laterally flattened anterior end of the ramus reaches a height of approximately

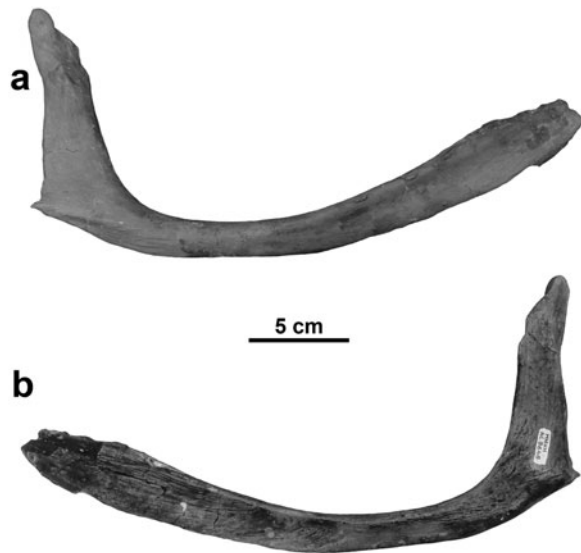


Figure 6. Jugal of MNHN AC 9648 in (a) right lateral view and (b) right medial view. Scale bar equals 5 cm.

two-thirds of the dorsal ramus. The medial surface of the element is generally flatter than the gently bowed lateral face, except for the shallow sulcus along the medial face of the anterior ramus where the jugal articulates with the lateral surface of the anterior ramus of the ectopterygoid (Fig. 6b).

3.a.8. Squamosal

The squamosal of MNHN AC 9648 is incomplete, but the preserved morphology is fairly typical of mosasaurs, bearing a long anterior shaft and terminating in broad articular facets (Fig. 7). The anterior shaft is mediolaterally compressed and bears a deep dorsal groove for the posterior process of the postorbitofrontal. In lateral view (Fig. 7a), the ventral border of the shaft is quite straight. Posteriorly, the dorsal border of the lateral wall of the shaft curves ventrally to contribute to the articular facets, but the shaft is somewhat offset from the squamosal body, forming a posteroventrally oriented lateral ridge (Fig. 7a, b). Ventrolaterally on the squamosal body, there is a concave facet, which is subtriangular in ventral view (Fig. 7d), for the articulation with the curved suprapedial process of the quadrate. In dorsal view (Fig. 7b), the body of the squamosal is slightly expanded laterally and more greatly expanded medially, giving this region of the bone an asymmetrical arrowhead outline. The groove for the postorbitofrontal begins just anterior to the widest part of the squamosal and deepens as the shaft narrows. The posteromedial edge of the squamosal body overlaps the posterolateral face of the supratemporal. In medial view (Fig. 7c), there is a shelf of bone that arises from the posterior termination of the squamosal and extends anterodorsally towards the shaft, which separates the articular facet for the supratemporal and the quadrate. The articular facet for the quadrate is concave vent-

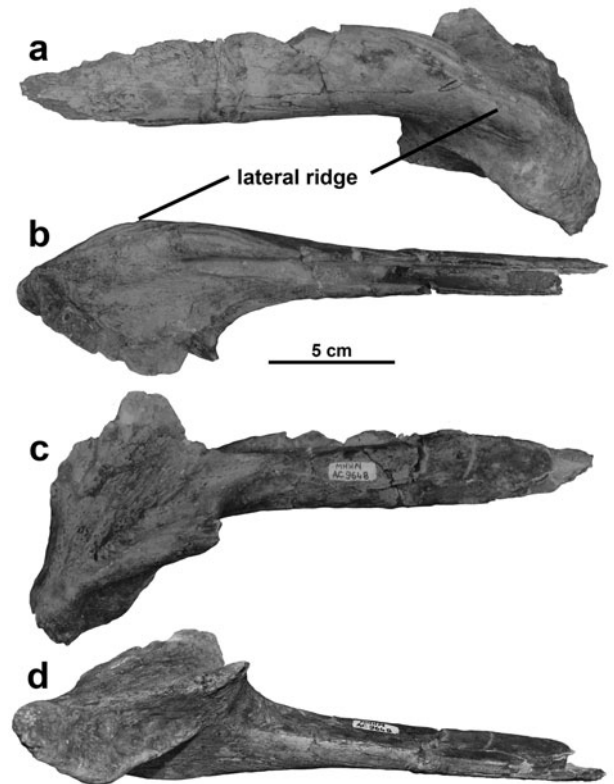


Figure 7. Squamosal of MNHN AC 9648 in (a) left lateral view, (b) left dorsal view, (c) left medial view, and (d) left ventral view. Scale bar equals 5 cm.

ral to this ridge, and posterodorsal to this ridge is the deep, triangular facet for the supratemporal. In ventral view (Fig. 7d), the squamosal shaft is rounded ventrally, and broadens gradually into the body of the squamosal posteriorly.

3.a.9. Palatine/vomer

The palatine of MNHN AC 9648 is crushed against the maxilla obscuring its morphology (Fig. 3b, c). Ventrally, the palatine is a flat plate of bone with a posterior triangular fossa for articulation with the anterior end of the pterygoid. A blunt ridge, most prominent medially, bounds this depression. Anteriorly there is a deep, U-shaped embayment surrounded by an anterolateral process, which is flat, broad and articulates with the maxilla directly above the tooth row from the posterior of the tenth tooth caudally, and a longer, narrower anteromedial process, which would articulate with its counterpart medially and with the vomer anterodorsal to the ninth maxillary tooth. It appears that a fragment of the vomer of MNHN AC 9648 is also preserved extending from the suture with the palatine anterior to the sixth maxillary tooth. The vomer is longitudinally concave medially, with narrow ridges dorsally and ventrally, to meet its counterpart on the midline.

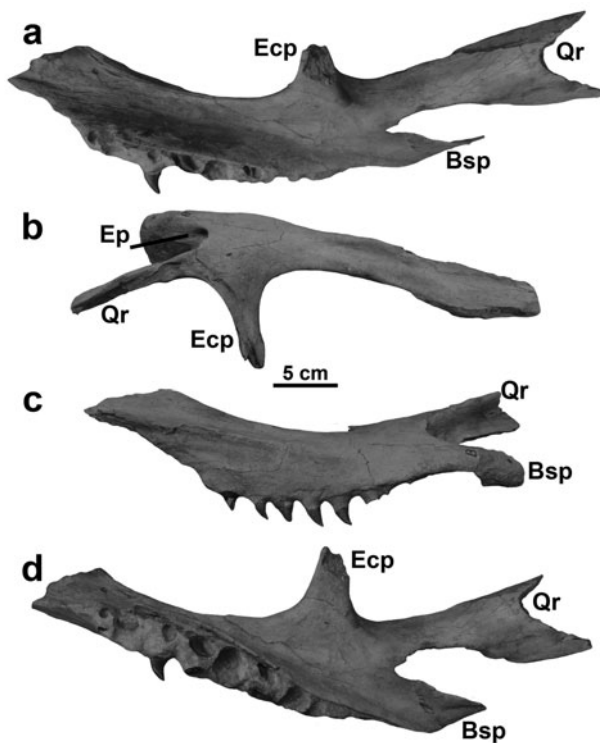


Figure 8. Pterygoid of MNHN AC 9648 in (a) left lateral view, (b) right dorsal view, (c) right medial view, and (d) left ventral view. Abbreviations: Bsp – basisphenoid process; Ecp – ectopterygoid process; Ep – epipterygoid pit; Qr – quadratic ramus. Note: letters visible on the fossil have been painted on the specimen and bear no association with the labelling system of this study. Scale bar equals 5 cm.

3.a.10. Pterygoid

The pterygoids of MNHN AC 9648 bear eight conical, posteriorly curved teeth (Fig. 8). The pterygoid teeth are smaller than the marginal teeth, but the teeth do slightly vary in size along the tooth row, being largest at the midpoint of the tooth row and the posterior pterygoid teeth being quite petite. Unlike the facets or prisms of the marginal teeth, the enamel of the pterygoid teeth is smooth and unornamented save for a faint posterior carina.

In ventrolateral view (Fig. 8a), the tooth row descends from the main body of the pterygoid on a robust flange. This flange is relatively tall (approximately twice the height of the pterygoid tooth crowns at its tallest point), and ventrally convex (Fig. 8c). Anteriorly the flange is nearly vertical, but posteriorly, as the flange tapers dorsally, it angles slightly medially.

Dorsally (Fig. 8b), the main body exhibits a medial ridge dorsal to the tooth row with a shallow sulcus lateral to the ridge. In medial view (Fig. 8c), the tooth-bearing flange descends from this medial ridge. This combination of ridge and sulcus does not extend along the main body to the anterior termination of the element and is most prominent dorsal to the anterior-most pterygoid teeth. There is a small foramen on the dorsal surface of the pterygoid, lateral to the main body of the element but anteromedial to the divergence of the ect-

opterygoid process and the quadratic ramus (Fig. 8b). The position of this foramen is variable. In MNHN AC 9648, the foramen is near the centre of the sheet of bone that connects the ectopterygoid process and the quadratic ramus, but in IRSNB R 26, the foramen is in the anterior edge of the fossa along the posterior margin of the ectopterygoid process. On the dorsal surface of the pterygoid, at the apex of the curve created by the divergence of the quadratic ramus and the basisphenoid process, is a round indentation, which is likely the epipterygoid pit. It is not perpendicular to the dorsal surface of the main body of the pterygoid but merges into the vertical surface spanning the socket between the two posterior processes.

The ectopterygoid process is sub-triangular in cross-section with a posteroventral keel that is offset from the pterygoid body (Fig. 8a). The posterior termination of the ectopterygoid process bears an elongate sulcus for articulation with the ectopterygoid (Fig. 8b). The ectopterygoid process diverges from the main body of the element at approximately a 75° angle, but the dorsal surface of the element is broad at this point, so the curve that forms between the ectopterygoid process and the main body is gentle. The posterior edge of the dorsal surface of the ectopterygoid process bears a shallow fossa with a distinct anterior edge, which continues across the base of the quadratic ramus.

The quadratic ramus is thin-walled and dorsomedially concave, giving it a U-shape in cross-section (Fig. 8a, c, d). The ramus is constricted posterior to its divergence from the main body of the pterygoid and the ectopterygoid process, but at a point even with, or posterior to the termination of the basisphenoid process, the quadrate ramus flares more broadly. The posterior end of the quadrate ramus is broken, so its complete length along with the nature of the articular surface for the quadrate is also unknown.

The main feature of the ventral side of the pterygoid (Fig. 8d) is the spindle-shaped tooth row. The parapets of the flange that border the tooth row are not parallel. Medially, the parapet is relatively straight, but the lateral parapet bows outwards to accommodate the larger teeth at the middle of the tooth row. This curvature forms a slightly enclosed channel between the descending flange and the ventral surface of the main body of the pterygoid.

The basisphenoid process is posteriorly directed and dorsoventrally compressed (Fig. 8d). Ventrally, the basisphenoid process is broad at its base and bears a small, oval foramen. A deep socket forms between the quadrate ramus and the basisphenoid process. This socket is usually described as accepting the basiptyergoid process of the basisphenoid (e.g. Russell, 1967), and in taxa such as *Platecarpus* in which the basiptyergoid processes are thin, laterally expanded wings, this is probably the case. However, in *M. hoffmannii* the basiptyergoid processes are short, blunt and anteriorly directed (see basisphenoid description in Section 3.a.12 below). Attempts to articulate the basiptyergoid processes firmly in this socket cause the

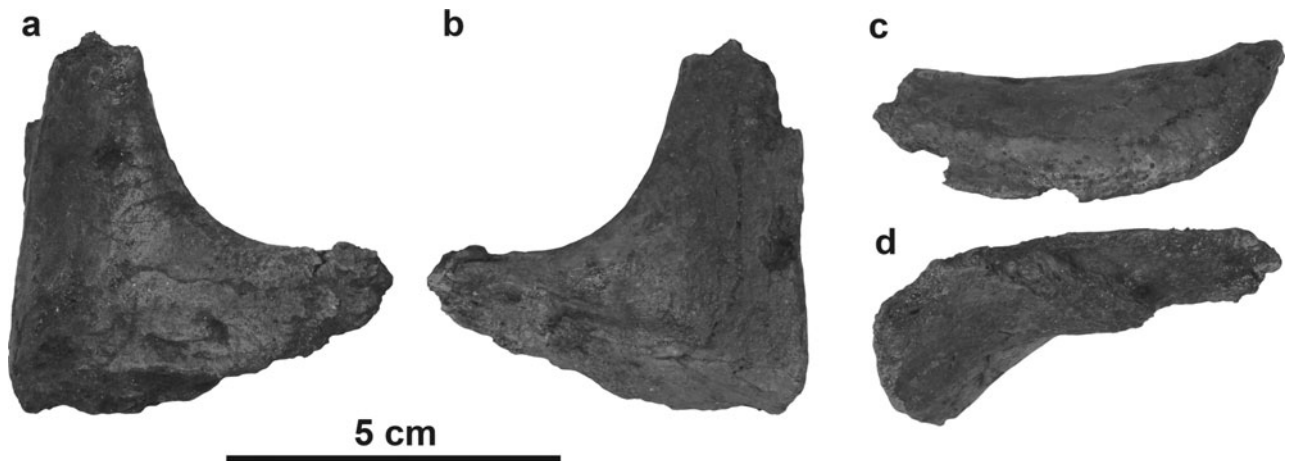


Figure 9. Ectopterygoid of AMNH 1389 in (a) left dorsal view, (b) left ventral view, (c) left lateral view, and (d) left posterior view. Scale bar equals 5 cm.

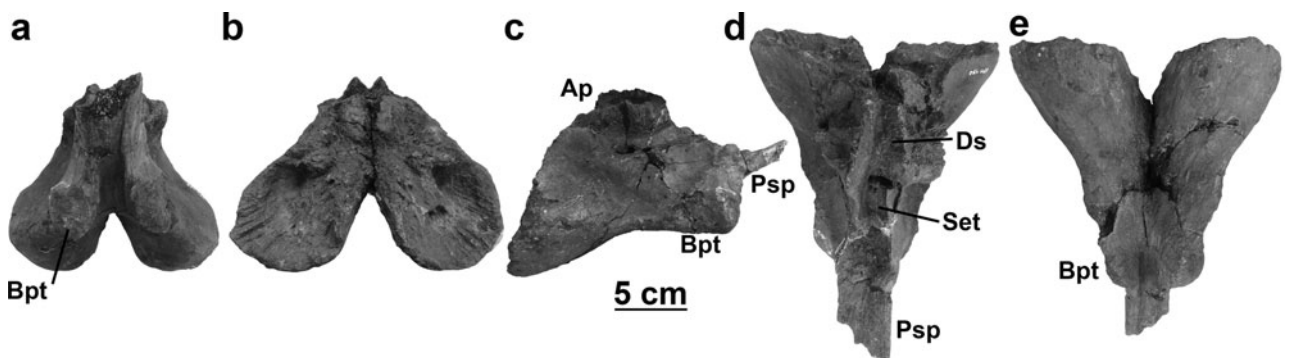


Figure 10. Basisphenoid of YPM 430 in (a) anterior view, (b) posterior view, (c) right lateral view, (d) dorsal view, and (e) ventral view. Abbreviations: Ap – alar process; Bpt – basipterygoid process; Ds – dorsum sellae; Psp – parasphenoid process; Set – sella turcica. Scale bar equals 5 cm.

basisphenoid processes of the pterygoids to cross at the midline. Therefore, the basisphenoid either only shallowly entered the socket between the quadratic ramus and the basisphenoid process, or perhaps it articulated only with the dorsal surface of the basisphenoid process, which is longitudinally concave dorsally. The socket between the two posterior processes of the pterygoid is confluent with the pit for the eipterygoid. The posterior, rather than dorsal, orientation of this pit indicates that the eipterygoid would have angled more posteriorly than dorsally, or even have been curved as is seen in *Plotosaurus* (LeBlanc, Caldwell & Lindgren, 2013) and *M. missouriensis* Harlan, 1834 (pers. obs.). The basisphenoid process tapers distally towards its termination ventral to the basisphenoid.

3.a.11. Ectopterygoid

No complete ectopterygoid is known for *Mosasaurus hoffmannii*, but from incomplete specimens (e.g. AMNH 1389), it appears this element has the L-shape typical of mosasaurs (Fig. 9a, b). The medial termination of the posterior ramus is incomplete, but the element narrows, likely to articulate with the sulcus at the

distal termination of the ectopterygoid process of the pterygoid. The posterior edge would have been straight to gently convex, and a shallow ridge parallels the border of the bone on the ventral surface (Fig. 9b). Between this ridge and the edge of the bone, the ventral surface slopes dorsally, likely serving as space for muscle attachment. The rest of the ventral surface of the ectopterygoid is flat, and the dorsal surface of the anterior ramus is convex dorsally. The lateral arm is also gently bowed ventrally, mirroring the curvature of the anterior arm of the jugal to which it articulated (Fig. 9c, d).

3.a.12. Basisphenoid

The only known braincase material for *Mosasaurus hoffmannii* comes from the Upper Maastrichtian greensands of New Jersey, from specimens previously assigned to *Mosasaurus 'maximus'*. The basisphenoid of YPM 430 (Fig. 10) preserves most of the salient characters of this element, lacking only some of the blood vessel and nerve foramina of the dorsal surface. The anterior end of the bone supports the anterodorsally extending parasphenoid process (Fig. 10a, c). This process is broadly V-shaped in cross-section.

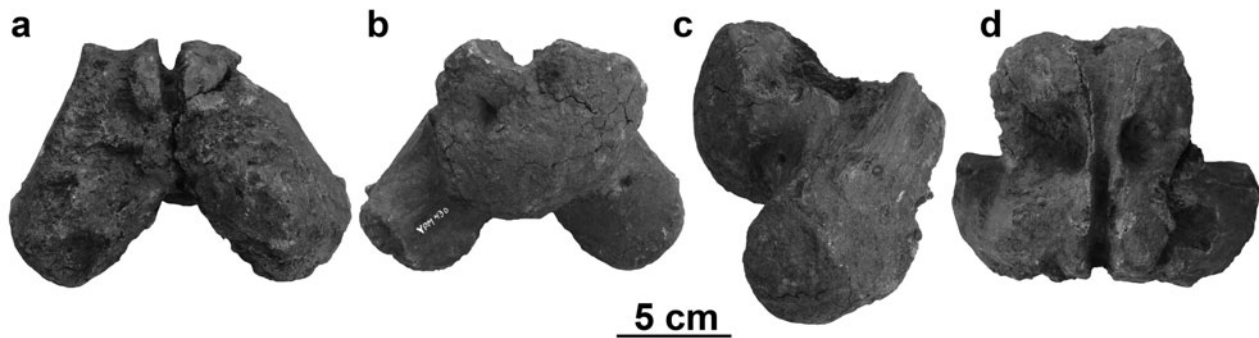


Figure 11. Basioccipital of YPM 430 in (a) anterior view, (b) posterior view, (c) right lateral view, and (d) dorsal view. Scale bar equals 5 cm.

Vertical sheets of bone connect the lateral surfaces of the parasphenoid process with the basiptyergoid processes that make up the anteroventral part of the element. In dorsal and ventral view (Fig. 10d, e), it is evident how reduced the basiptyergoid processes are in *Mosasaurus hoffmannii*. Rather than having the tetraradiate morphology described by Russell (1967), in this species the basisphenoid tapers anteriorly, and the basiptyergoid processes, instead of being laterally divergent, form rounded shoulders on either side of the parasphenoid rostrum. The basiptyergoid processes bear elliptical facets anteriorly, where the basisphenoid articulates with the pterygoid. This extreme reduction of the basiptyergoid processes appears to be unique to *M. hoffmannii*, though other taxa, including *Clidastes*, *M. lemonnieri* Dollo, 1889 and *M. mokoroa* Welles & Gregg, 1971 also exhibit reduced divergence of the basiptyergoid processes. The sockets between the basisphenoid processes and quadrate rami of the pterygoids are not correspondingly close-spaced, so it is possible that the basiptyergoid processes were capped in cartilage to bridge the space or that the articulation between these bones was not as tight (see pterygoid description in Section 3.a.10 above).

The basisphenoid is much wider posteriorly, where it bears two broad lobes that articulate with the basal tubera of the basioccipital (Fig. 10b). These articular facets are separated from each other ventrally by the extension of the midline fissure. The surfaces of the articular facets are striated, but whether these ridges supported a cartilaginous meniscus between the basisphenoid and basioccipital or formed an interlocking suture with similar ridges and grooves on the basioccipital is unclear owing to the poor surface preservation of the latter element. The articular facets of the basisphenoid also bear pits and foramina for the passage of nerves and blood vessels. The articular facets for the basal tubera of the basioccipital are not only wider than the basiptyergoid processes, but they also extend further ventrally (Fig. 10c).

The ventral lateral margins of the basisphenoid are gently sinusoidal, with an additional lateral expansion between the maximum width of the articular facets for the basal tubera of the basioccipital and the ba-

siptyergoid processes (Fig. 10d, e). A midline fissure that extends the entire ventral length of the bone separates the two basiptyergoid processes anteriorly and the two articular facets for the tubera of the basioccipital posteriorly.

In anterior view (Fig. 10a), it is evident that the dorsal alar processes of the basisphenoid are also reduced and only slightly overhang the lateral walls of the bone, but the lateral surfaces of the basisphenoid are longitudinally concave between the alar processes and the four ventral processes. Ventral to the mid-length of the alar process, two elliptical foramina pierce the lateral surface of the basisphenoid (Fig. 10c). A channel extends anteriorly from these foramina, just ventral to the alar process. These foramina and the channel likely supported blood vessels, including the internal carotid artery and the internal jugular, and nerves such as the facial nerve (Russell, 1967). Dorsally, the alar processes diverge around the posteriorly tapering dorsum sellae and the poorly preserved sella turcica (Fig. 10d). Two sets of foramina pierce the posterior portion of the sella turcica, possibly for branches of the basilar arteries or internal carotid arteries, and cranial nerve VI likely exited the basisphenoid through anteriorly directed foramina in the anterior edge of the alar process, each of which expand laterally to form complex surfaces for the articulation with the prootic dorsally.

3.a.13. Basioccipital

The basioccipital of YPM 430 is weathered and slightly deformed, but the overall morphology of the bone is preserved (Fig. 11). Anteriorly, the basioccipital is bifurcated into two oblong, convex basal tubera that articulate with the posterior facets of the basisphenoid (Fig. 11a). The surface of these tubera is uneven in YPM 430, but whether this reflects the condition of the element in life or the preservation of the fossil is unclear. The ventrolaterally directed basal tubera are relatively long and diverge from each other at an angle of approximately 80°. Each of the tubera is concave dorsally, and they are separated by a dorsal cleft for the medulla. The canal for the medulla is deep and narrow anteriorly, where its path lies dorsal to the basal tubera

(Fig. 11d). Posteriorly, this canal widens to form the floor of the foramen magnum.

Posteriorly, the basioccipital is dominated by the semicircular occipital condyle (Fig. 11b). The flat, dorsolateral surfaces of the occipital condyle articulate with the exoccipital processes, which in mosasaurs are fused to the opisthotic. In lateral view, the gently convex occipital condyle projects further posteriorly than the distal ends of the basal tubera (Fig. 11c).

Posterior to the basal tubera, the dorsal surface of the basioccipital bears two deep, oval pits on either side of the medullary canal (Fig. 11d). It is unlikely that these pits are homologous to the bilobate foramen for the basilar artery seen in the floor of the medullary canal of *Platecarpus*, both because these pits are borne in the articular facets for the opisthotic and also because there is no evidence of additional foramina on the anterior surface of the element where the artery would exit. These pits could have accepted a rounded ventral process from the opisthotic to form a more tightly interlocking suture, but the poor preservation of isolated opisthotics makes it difficult to support this supposition. It is posterior to these pits that the medullary canal broadens to become the foramen magnum. Lateral to the medullary canal are the broad surfaces that would have articulated with the prootic anteriorly and the opisthotic posteriorly.

3.a.14. Paroccipital bar

Connecting the basisphenoid and basioccipital medially with the squamosal and quadrate laterally is a robust bar of bone composed of the opisthotic, prootic and supratemporal (Fig. 12). As is the case across Mosasauridae, the exoccipital is completely fused to the posterior of the opisthotic in *Mosasaurus*. Medially, the prootic and opisthotic are complexly expanded to form the lateral walls of the braincase and house the otic capsule. The supratemporal bridges the gap between the lateral expansions of these braincase elements, the suspensory ramus of the parietal, the body of the squamosal and the suprastapedial process of the quadrate.

In anterolateral view, the paroccipital bar is dominated by the prootic ventrally and the supratemporal dorsally (Fig. 12a, b). An edge of the opisthotic bearing the protruding, blunt exoccipital is visible on the posterior surface. The prootic bears a ventral pedestal that articulates with the alar process of the basisphenoid anteriorly and the basioccipital posteriorly. This pedestal is constricted dorsally where it merges with the rest of the bone by the deep notch for the trigeminal nerve anteriorly and the internal auditory meatus posteriorly. The posteromedial surface of the pedestal to the alar process of the basisphenoid is indented by an anteromedially directed V-shaped notch, and the foramen for the exit of cranial nerve VII is located on the medial wall. A lateral crest that bounds this notch hides this foramen from lateral view (Fig. 12e, f). Dorsal to the notch for the trigeminal, a horizontal wedge of bone

projects anteriorly to support the descending process of the parietal. A third ramus of the prootic extends posterodorsally, along the paroccipital process of the opisthotic (POPR), to articulate with the supratemporal in an interdigitating suture around the mid-length of the shaft of the paroccipital bar.

Dorsal to this suture, the supratemporal expands anteriorly and posteriorly to support articular structures for the squamosal and quadrate (Fig. 12a, b). The body of the supratemporal is bisected by a deep groove that originates near the posterior edge of the bone and curves dorsally, and which accepts the similarly curved medial shelf of the squamosal. Dorsal to this groove is a broad, anteriorly projecting triangular process that corresponds with the concave facet dorsal to the medial shelf of the squamosal. Ventral to the groove is a less-pronounced ridge surrounding a deep vertical depression. This depression likely accepts the medial expansion of the suprastapedial process of the quadrate. The anterior of the depression for the suprastapedial process is bounded by a posteroventrally directed projection, which is bracketed by a pair of pits or wide foramina dorsally and ventrally. An additional process, which is flat dorsally and keeled ventrally resulting in a triangular cross-section, extends anteromedially to meet the posterior ramus of the parietal (Fig. 12c, d). Between the lateral process for the squamosal and the medial process for the suspensory ramus of the parietal the supratemporal extends ventrally, wrapping around the distal termination of the POPR. In ventral view (Fig. 12e, f), the distal termination of the supratemporal is triradiate, with the vertical bar of bone, which accepts the medial projection of the suprastapedial process, extending ventrally between the two dorsal processes (the process to articulate with the posterior ramus of the parietal posteromedially, and the squamosal process anterolaterally). Dorsally, the body of the supratemporal is perforated by widely spaced foramina (Fig. 12g, h). The margin of the triangular squamosal process is convex posteriorly to slot into the groove dorsal to the medial shelf of the squamosal. The termination of the supratemporal is saddle-shaped in dorsal view, where the vertical bar, which is overlapped by the dorsal edge of the squamosal, merges into the ascending posteromedial process to the posterior ramus of the parietal, which is offset from the dorsal plane of the main body of the supratemporal by a sharp groove.

In dorsomedial view (Fig. 12c, d), the paroccipital bar is dominated by the paroccipital process of the opisthotic. The posterior portion of the parietal process of the prootic is deeply striated to articulate with the supraoccipital (Fig. 12c). This depressed articular surface is saddle-shaped and continues posteriorly onto the POPR to a point even with the exoccipital process, though the opisthotic is less deeply grooved than the prootic (Fig. 12c, g, h). The middle of the articular surface for the supraoccipital is penetrated by a large pit for the utriculus. The utriculus is supposed to lie in the suture between the prootic and the

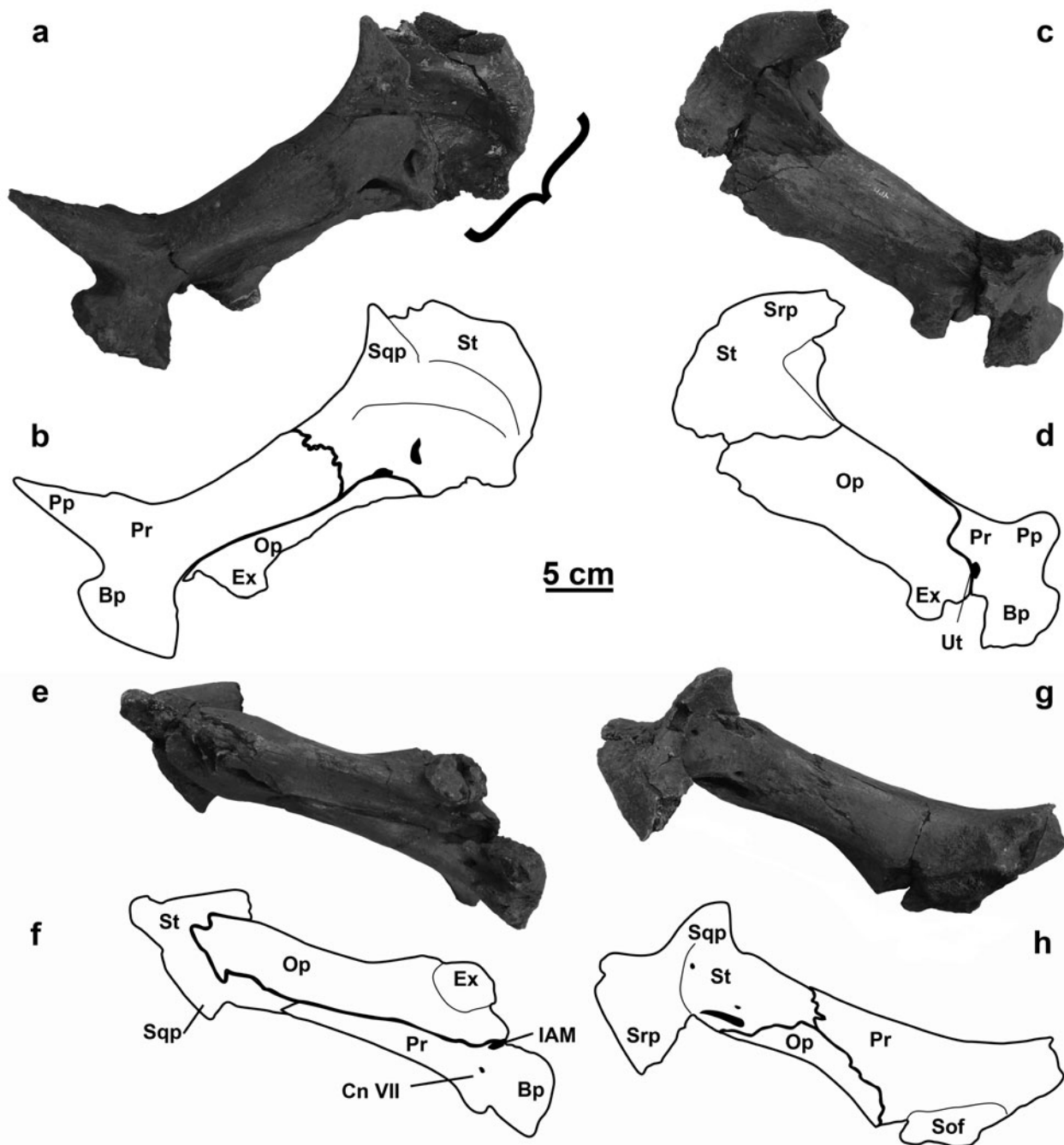


Figure 12. Paroccipital bar. (a) YPM 430 right (reflected for consistency) composited with YPM 1504 left (bracketed region) in anterolateral view and (b) the same outlined to indicate bone sutures and processes. (c) YPM 430 left in posterodorsal view and (d) the same outlined to indicate bone sutures and processes. (e) YPM 430 left in ventral view and (f) the same outlined to indicate bone sutures and processes. (g) YPM 430 left in dorsal view and (h) the same outlined to indicate bone sutures and processes. Abbreviations: Bp – pedestal to basisphenoid; Cn VII – cranial nerve VII; Ex – exoccipital; IAM – internal auditory meatus; Op – opisthotic; Pp – parietal process; Pr – prootic; Sof – facet for supraoccipital; Sqp – squamosal process; Srp – suspensorial ramus process; St – supratemporal; Ut – utriculus. Scale bar equals 5 cm.

opisthotic, which is oriented nearly vertically in taxa like *Clidastes* (Russell, 1967), but the left paroccipital bar of YPM 430 is fractured through the utriculus and the base of the supraoccipital covers the articular surface of the right paroccipital bar of the same specimen. The typical position of the utriculus is observed in a large, isolated paroccipital bar from the Hornerstown Formation of New Jersey (NJSM 11895). This speci-

men is listed as an indeterminate mosasaur, but the size and proportions of the element compare favourably with *M. hoffmannii*. Foramina for the semicircular canals pierce the prootic and opisthotic on either side of the utriculus of NJSM 11895. Lateral to the utriculus is a shallow depression between the prominent exoccipital process and a low ridge that extends posterolaterally from the edge of the articular surface for the

supraoccipital to the lateral termination of the POPR (Fig. 12c). A cluster of foramina pierces the POPR on, or anterior to, this ridge. The POPR curves slightly anteriorly where it meets the prootic medially and the supratemporal laterally, but otherwise the paroccipital bar is relatively flat in this view. The fused exoccipital is a short, blunt process that projects nearly perpendicularly from the posterior surface of the POPR. The ventromedial faces of the exoccipital would articulate with the dorsolateral edges of the occipital condyle.

In posteroventral view, the medial, and to a lesser degree, the distal ends of the paroccipital bar are expanded, giving the middle of the bar a slightly constricted appearance (Fig. 12e, f). The proximal expansion is caused by various articular structures including the anterior ramus for the descending process of the parietal dorsally, the pedestal to the basisphenoid anteroventrally and the blunt exoccipital posteroventrally. The articular surface of the exoccipital is elliptical from this view and rugose. A deep, rounded-bottomed groove separates the exoccipital and the ventral pedestal and extends the entire length of the paroccipital bar, becoming shallower distally. In life, this groove would likely have housed the columella to transfer sound vibrations from cartilaginous structures supported by the quadrate to the structures of the inner ear through the internal auditory meatus at its ventromedial termination. The suture between the prootic and the POPR lies along the anterior of this groove, and the prootic tapers distally to its interdigitating suture with the supratemporal. Between this groove and the exoccipital process, there is the base of a third process that was not preserved completely. This is likely the base of a thin sheet of the opisthotic that would have extended ventrally along the posterior surface of the basal tuber of the basioccipital and borne the foramina for the exit of cranial nerves IX–XII. Distally, a ventral projection of the supratemporal splits the end of the POPR. This projection of the supratemporal forms a U-shaped lip that locks the distal end of the POPR in place. The larger, flat surface of the POPR wraps around the medial surface of this lip to terminate further distally along the supratemporal. It also appears that a channel extended through the inside of the paroccipital bar between the anterior edge of the POPR and the supratemporal.

From the posterior corner of the supraoccipital, the border of the prootic extends anteriorly, along the POPR proximally and the supratemporal distally (Fig. 12g, h). The POPR makes only a minor, arched contribution to the posterior of the dorsal surface of the paroccipital bar between the prootic and supratemporal. This is partially owing to the state of preservation, and in life the POPR would have extended further distally, filling in a posterior concavity along the margin of the supratemporal. Because the POPR is incomplete distally, a channel is visible between the POPR and the supratemporal, likely confluent with the similar channel observed from the ventral view. The ridge that bounds the anterior of the canal to the utriculus is visible as a posterior expansion.

3.a.15. *Quadrate*

Unlike the conditions seen in other lineages of mosasaurs, such as *Clidastes* or *Platecarpus*, the quadrate of *Mosasaurus hoffmannii*, as exemplified by MNHN AC 9648, is actually relatively quadrilateral, particularly the lateral and the anterior faces (Fig. 13a, b). The quadrate is tall for its anterior–posterior length. In lateral view, pronounced dorsal and ventral corners mark the anterior edge of the tympanic rim, and the mandibular condyle is offset from the ventral margin of the alar wing. The anterior and ventral rims of the tympanic ala are marked with a distinct groove. The outer border of this groove is broader than the inner edge, which also traces a gentler curve than the outer corner. Most specimens are worn in this area, but it appears that this groove terminates at a point even with the mandibular condyle and would not have continued around the tympanic rim. At the posteroventral corner, the tympanic rim narrows and projects laterally to form a thin flange, which angles dorsomedially and terminates directly ventral to the suprastapedial process. A broken region at the dorsal termination suggests that the flange would have been free of the main shaft at its tapered distal extremity. The suprastapedial process is short and tightly curved around an oval stapedial notch. The cephalic condyle is dorsally convex in lateral view and continues posteriorly along the outer surface of the proximal half of the suprastapedial process forming the articular facet for the squamosal as described by Konishi & Caldwell (2011).

In anterior view (Fig. 13b), the quadrate is quite quadrilateral, narrower dorsally than ventrally, and with a medial projection that is the distal end of the suprastapedial process. The middle of the dorsal edge of the alar wing is indented by a U-shaped depression, likely corresponding to the inverted triangular depression Russell (1967) interpreted as the origin of the adductor mandibulae externus profundus muscle. The mandibular condyle is ventrally convex and laterally expanded, twisting the ventral region away from the plane formed by the tympanic ala. This portion of the anterior surface of the quadrate is concave from the anteroventral corner of the tympanic rim to the medial flange of the quadrate shaft. The medial border of the alar wing, where it merges with the shaft is marked by rugosities. One of these forms a low broad ridge along the middle third of the height of the shaft, where the alar wing merges with the main shaft. This ridge originates anterior to the stapedial pit and extends ventrally, terminating just dorsal to the offset area of the mandibular condyle and was likely the attachment site for the adductor mandibulae posterior muscle (Russell, 1967).

The quadrate is narrowest in medial view (Fig. 13c). The dorsal edge of the element in this view is formed by the smooth arc of the ventrally curving suprastapedial process. The dorsal region of the main shaft is concave, forming a large fossa that articulates with the supratemporal. Directly ventral to the dorsal fossa is the oval stapedial pit. The long axis of the pit is

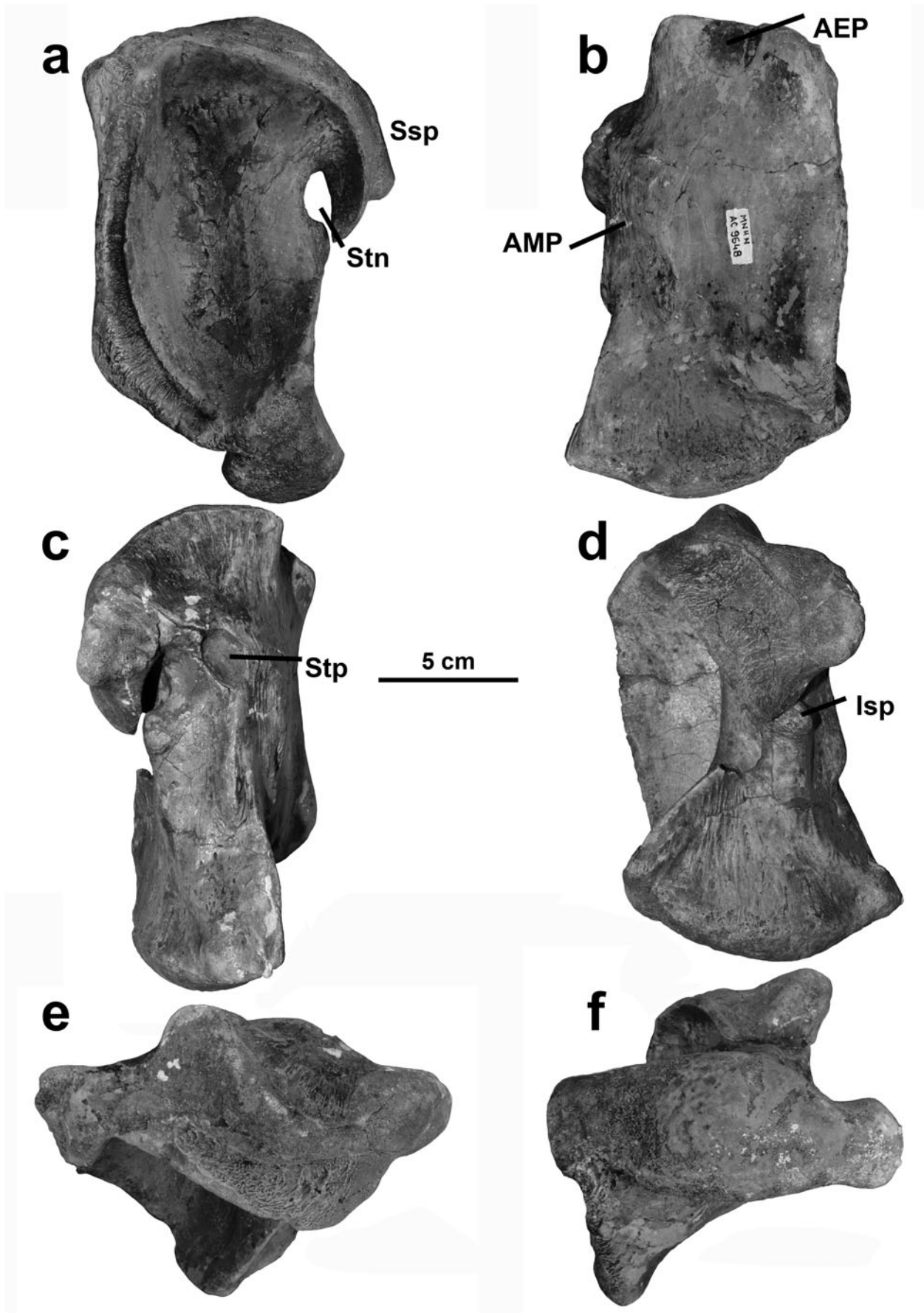


Figure 13. MNHN AC 9648 quadrate in (a) left lateral view, (b) left anterior view, (c) left medial view, (d) left posterior view, (e) left dorsal view, and (f) left ventral view. Abbreviations: AEP – attachment site for adductor mandibulae externus profundus muscle; AMP – attachment site for adductor mandibulae posterior muscle; Isp – infrastapedial process; Stn – stapedial notch; Stp – stapedial pit; Ssp – suprastapedial process. Scale bar equals 5 cm.

oriented at approximately a 30° angle from the vertical axis of the main shaft. A second ridge (Fig. 13c), more robust than the low rugose ridge on the anterior face of the element, originates from the ventral end of the stapedial pit and also extends ventrally. This ridge broadens slightly at its ventral termination, and a finer crest of bone extends from the anterior side of the ridge that continues ventrally to merge with the mandibular condyle. The infrastapedial process, a large posterior protuberance, forms the ventral border of the stapedial notch. The distal end of the suprastapedial process almost contacts the lateral edge of the infrastapedial process. The slope of the protuberance to the shaft is much steeper dorsally where it contributes to the stapedial notch, but the slope grades more gradually into the shaft ventrally. The ventromedial edge of the infrastapedial process is indented by a shallow groove, rather than being smoothly confluent with the shaft as is seen around the rest of the process.

The medial expansion of the suprastapedial process can be seen in posterior view (Fig. 13d). The lateral side of the process is occupied by a rugose fossa, while a broad round projection extends from the medial edge to articulate with the supratemporal. The ventral end of the shaft, where it forms the mandibular condyle, is expanded medially and laterally, forming an elongated, ventrally convex articular surface. The ascending distal crest of the tympanic rim angles towards the infrastapedial process and the termination of the suprastapedial process.

The chephalic condyle is quite convoluted (Fig. 13e). Two fossae invade the articular surface from the anterior and the medial faces that interrupt what might otherwise be a broadly spindle-shaped condyle similar to the ventral condition. The more anterior of these fossae is the U-shaped insertion for the adductor mandibulae externus profundus as described above, whereas the medial fossa is considerably broader and contributed to the articulation with the supratemporal. The cranial condyle is also more rugose than the mandibular, particularly the lateral fossa that begins dorsal to the tallest corner of the tympanum and curves posteriorly and ventrally around the suprastapedial process.

The long axis of the ventral condyle is oriented mediolaterally and is convex ventrally (Fig. 13f). The condyle is broadly spindle-shaped, being widest where it intersects the shaft. The condyle tapers slightly and evenly laterally but is more sharply constricted medial to the shaft and expands again slightly before its blunt medial termination. The mandibular condyle is nearly perpendicular to the lateral face of the quadrate conch, and the ventral edge of the tympanic ala is correspondingly pulled laterally.

3.a.16. Dentary

The dentaries of MNHN AC 9648 are long, straight, robust and bear 14 tooth positions (Fig. 1). The ventral margin in particular lacks curvature, and the tooth margin is only very gently dorsally concave. The dent-

ary is bluntly rounded anterior to the first tooth, and the height gradually increases posteriorly. The lateral surface is perforated by nutrient foramina. Anteriorly, even with the first six dentary teeth, the foramina are more densely clustered and cover much of the dorsolateral extent of the bone, and posteriorly the foramina are more widely spaced and form a single row. Medially, the dentary bears a longitudinal groove that widens posteriorly to accept the splenial and the anterior ramus of the articular. There is a large foramen in the dorsal border of this groove ventral to the eleventh dentary tooth. The medial parapet bounding the tooth row is approximately as high as the lateral parapet. The teeth are relatively similar in size, with the anterior teeth being slightly smaller than most of the teeth in the middle of the dentary, and the posterior teeth being the smallest.

The holotype specimen also displays a few pathologies. Ventral to the tenth and eleventh teeth of the left dentary are a pair of gouges, each surrounded by varying degrees of rugose, secondarily remodelled bone. It appears that this individual was the victim of a biting attack from another large, toothed animal, presumably another mosasaur, but survived the encounter and underwent healing at the bite site. Additionally, the anterior portions of the dentaries are unexpectedly rugose. Some degree of rugosity is expected on the medial surface where the dentaries meet on the midline to form the ligamentous dental symphysis, but in this specimen, the rugosity wraps ventrally around to the lateral face of the elements as well. This region is marked by pits and bulges of remodelled bone that do not extend past the first tooth position. The anterior termination of the dentary would be an unlikely place for a fracture, unless *M. hoffmannii* utilized its lower jaw in some sort of ramming behaviour, so it seems more probable that this pathology was caused by damage to the ligaments binding the intermandibular joint together.

3.a.17. Splenial

The splenial lies medial to the dentary, and while tall medially (Fig. 14a, b), laterally the splenial is only visible as a narrow wedge that begins ventral to the twelfth dentary tooth and widens posteriorly towards its termination at the intramandibular joint (Figs 1, 14c). The splenial forms the posterior-most extent of the anterior half of the lower jaw and terminates in a concave cotyle to receive the angular. Isolated, the splenial is long and V-shaped in cross-section, with a robust base and two thin dorsal wings. The lateral wing is formed by a depressed fossa that serves as the articular facet for the dentary. A distinct straight shelf forms the ventral edge of this fossa where the dentary overlaps the splenial, marking the division between the thin lateral wing and the robust wedge of bone ventral to the dentary. The medial wing is taller than the lateral wing and rises as a smooth face from the base of the splenial (Fig. 14b). The medial ramus of the splenial extends anteriorly along the groove in the dentary to a point ventral to the posterior side of the fifth dentary tooth in MNHN

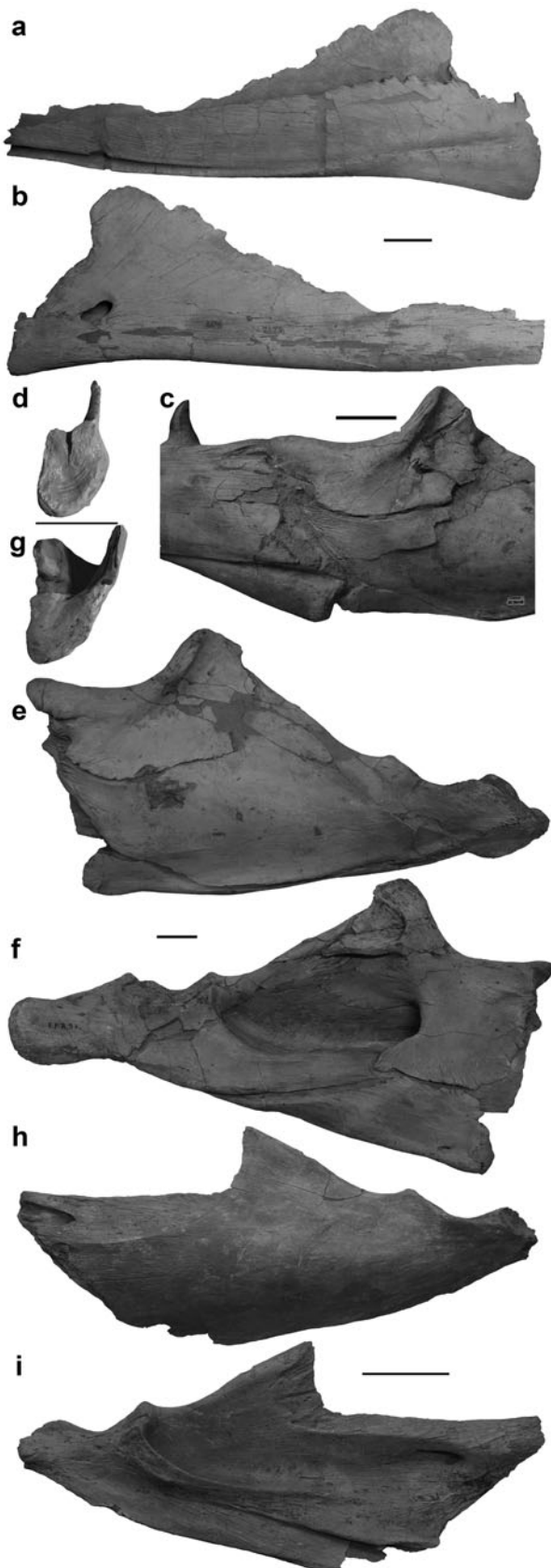


Figure 14. Lower mandibles. (a, b) Splenial of IRSNB R 302 in (a) left lateral view and (b) left medial view. (c) Intramandibular joint of MNHN AC 9648 in left lateral view. (d) Splenial of IRSNB R 26 in posterior view. (e–g) Post-dentary unit of IRSNB R 24 in (e) left lateral view, (f) left medial view, and (g) angular in anterior view. (h, i) Surangular of IRSNB R 301 in (h) left lateral view and (i) left medial view. Scale bars equal 5 cm.

AC 9648, where it ends in a blunt point (Fig. 1). It is likely that this part of the splenial is worn or broken, but it is unlikely that the splenial would have continued much further anteriorly considering that the anteriorly complete splenial of IRSNB 1503 terminates even with the anterior side of the fifth tooth. The medial wing of the splenial increases in height posteriorly, gradually anterior to, and more steeply posterior to the foramen in the dentary that invades its dorsal border ventral to the eleventh tooth. Near the posteroventral corner of the splenial, ventral to the tallest point of the medial wing and approximately even with the posterior termination of the dentary in median view, it is perforated by an oblong foramen. The deep groove between the wings accepts the anterior extension of the prearticular.

Posteriorly, the articular facet of the splenial of IRSNB R 26 is D-shaped with straight internal and laterally convex external surfaces (Fig. 14d). The ventral portion of the articular surface is concave to accept the angular, but the joint surface is more complex dorsally. Confluent with the lateral wing of the splenial, a blunt wedge of bone projects posteriorly from the articular surface. Medial to this wedge the dorsal border of the articular facet is concave. The angular has corresponding features to form the intramandibular joint.

3.a.18. Angular

The angular forms the anteroventral margin of the post-dentary unit (Fig. 14c, e, f). The ventral margin is straight, and the dorsal margin, where the angular and the surangular meet, is slightly more irregular. The angular decreases in height gradually for the anterior three-quarters of its length, and tapers more steeply posteriorly. Owing to this tapering, the angular is only laterally visible for the anterior quarter of the post-dentary unit ventral length.

The angular contributes to a greater proportion of the post-dentary unit in medial view (Fig. 14f). Medially, the angular is visible as a posteriorly tapering wedge of bone that forms the ventral margin of the anterior half of the post-dentary unit. The dorsal border of the angular articulates with the prearticular, but the anteromedial wing of the coronoid overlaps the prearticular to contact the anterior half of the angular.

The morphology of the anterior surface of the articular facet corresponds with the concavities and processes of the splenial (Fig. 14g). Similar to the splenial the internal surface of the angular is vertical and the external surface is laterally bowed. The ventral portion of the angular articular surface is anteriorly convex, and the dorsal portion is indented by a median notch to accept the wedge-shaped process from the splenial.

3.a.19. Surangular

The surangular contributes to most of the lateral surface of the post-dentary unit of MNHN AC 9648 (Fig. 14e, h). It participates in the intramandibular joint along with the coronoid and the angular. The lateral surface

of the surangular is convex. The surangular is tallest at about the midpoint of the length of the post-dentary unit, where it expands slightly ventrally and significantly dorsally, around the posterior terminations of both the angular and the coronoid. Posteriorly, the surangular rapidly decreases in height. The ventral border slopes evenly dorsally to suture with the articular, whereas the thin dorsal border is much more sinuous. As the coronoid buttress descends towards the glenoid fossa, the ventral trend of the border is interrupted by two dorsal eminences. The anterodorsal eminence is less pronounced than the eminence directly anterior to the glenoid fossa. The surangular contributes to the anterolateral margin of the glenoid fossa, and posterior to the glenoid fossa the surangular tapers to a wedge, where it is embraced by the articular dorsally and ventrally.

Medially, the surangular is visible dorsal to the prearticular and posterior to the coronoid where it forms the lateral wall of the adductor fossa (Fig. 14f, i). A channel pierces the anterior extension of the surangular on which the coronoid sits. This channel is usually obscured both medially and laterally by the descending wings of the coronoid, but it angles anterolaterally to exit the surangular along the anteroventral margin of the coronoid.

3.a.20. Coronoid

The coronoid forms the anterodorsal border of the post-dentary unit where it articulates with the dorsal margin of the surangular (Fig. 14c, e, f). The coronoid of MNHN AC 9648 is the typical saddle shape seen in mosasaurs, with lateral and medial wings embracing the surangular and a dorsally expanded posterior coronoid process. This posterior process is quite tall and mediolaterally thickest at its anterior margin, where it is also marked by a cluster of parallel, longitudinal grooves. Posteriorly, the ascending coronoid process is sharply indented by a sulcus that originates at the highest point of the coronoid and follows a similar curve to the anterodorsally concave margin of the coronoid and extends ventrally onto the lateral wing, forming a broad fossa. The ventral border of the coronoid is generally ventrally curved, but the anterior margin is interrupted by a deep embayment. This C-shaped excavation corresponds with the exit of the channel that pierces the anterior extent of the surangular. The posteroventral margin is irregularly scalloped, and the posterior margin forms a smooth curve.

In dorsal view, the anterior of the coronoid is bifurcated, and the lateral wing is anteriorly longer than the median wing. The anterior lateral wing is also dorsally more convex than the median wing. Medially, the coronoid of IRSNB R 24 is composed of a dorsal wing extending posteriorly from the coronoid process and an anteromedial wing extending ventrally from the saddle of the coronoid. The anteromedial wing extends further ventrally than the lateral wing, but rather than extending the entire length of the element, the anteromedial wing is separated from the dorsomedial wing by a deep U-

shaped embayment approximately even with the dorsal inflection of the coronoid process. Ventrally, the anteromedial wing of the coronoid contacts the angular. This suture is straight for most of its length, but the anteromedial wing bears a posterior projection that forms a slight hook, which allows for contact between the coronoid and the angular where the angular begins to taper ventrally.

3.a.21. Articular

As is the case across Mosasauridae, the articular and prearticular are fused into a single unit that is sutured to the surangular laterally and the angular ventrally. The only portions of the articular of MNHN AC 9648 that are visible in lateral view are the retroarticular process and a thin blade of bone that borders the posteroventral termination of the surangular (Fig. 1). The glenoid fossa is oriented obliquely mediolaterally, and the articular contributes to the medial and posterior borders of the fossa (Fig. 14e). The retroarticular process is rotated laterally, so that its maximum dimension is not vertical but rather obliquely mediolateral. Therefore, the lateral profile of the retroarticular process is not large and round as is seen in other groups of mosasaurs but instead appears to be dorsoventrally compressed.

Medially, the retroarticular process is slightly depressed by a shallow dorsal concavity, but the edges of the process provided attachment sites for muscles including the depressor mandibulae (Fig. 14f). The articular is tallest where it contributes to the glenoid fossa; this increase in height is achieved by a dorsal expansion of the unit posterior to the glenoid and a ventral expansion even with the glenoid. Anterior to the glenoid, at the posterior-most contact between the articular and the angular, the ventral margin of the articular ceases to angle further ventrally. In *Mosasaurus hoffmannii* the dorsal border of the prearticular slopes ventrally to correspond with the floor of the adductor fossa formed by the surangular and continues anteriorly to be sandwiched between the surangular and the anteromedial wing of the coronoid dorsal to the angular.

3.a.22. Teeth

The marginal teeth of MNHN AC 9648 are large, faceted and bear two carinae, which are very finely serrated (Figs 1–3). They are slightly curved posteriorly and round with little to no mediolateral compression. Anteriorly, the carinae are oriented at an acute angle to each other, making the labial circumference between the carinae considerably shorter than the lingual circumference. Therefore, in the anterior maxillary teeth the lateral face of each tooth is nearly flat between the anterior and posterior carinae. In the dentary teeth, this short, flat face is directed anterolaterally because the posterior carina is oriented along the lateral side of each tooth. The posterior carina shifts position to a more truly posterior orientation around the middle of

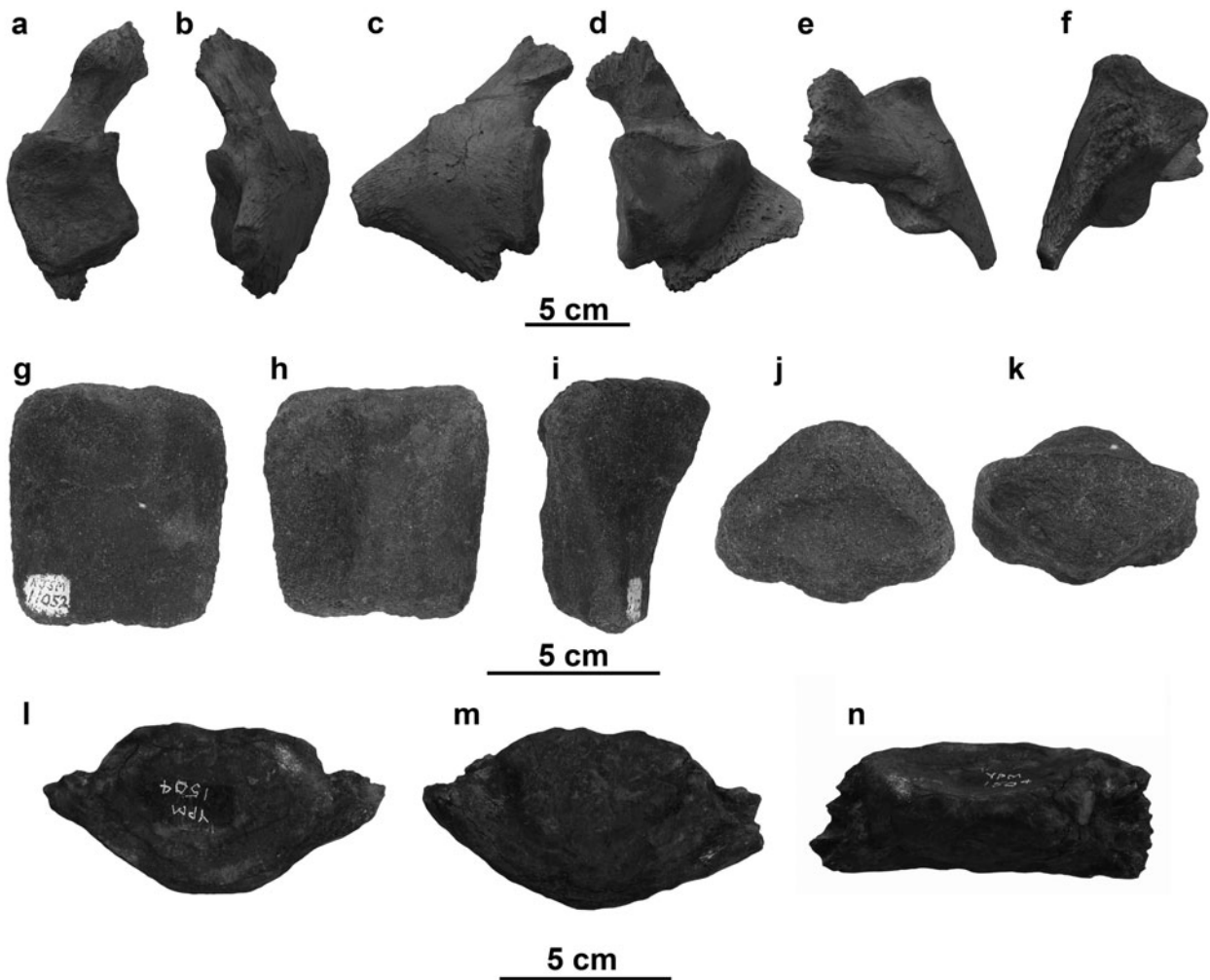


Figure 15. Right atlas neural arch of IRSNB R 300 in (a) anterior view, (b) posterior view, (c) lateral view, (d) medial view, (e) dorsal view, and (f) ventral view. Atlas centrum of NJSM 11052 in (g) anterior view, (h) posterior view, (i) right lateral view, (j) dorsal view, and (k) ventral view. Atlas intercentrum of YPM 430 in (l) anterior view, (m) posterior view, and (n) dorsal view. Scale bars equal 5 cm.

the tooth row. The tooth roots are long and thick. From the base of the crown, the root flares outwards to form a distinct shoulder. The root can be slightly curved, continuing the curvature of the crown, and the sides of the root taper only slightly along their length.

The number and size of facets formed by the enamel of the marginal teeth have been used to diagnose species of *Mosasaurus* since the genus was first described. While most species of *Mosasaurus* do display some sort of enamel ornamentation, *M. conodon* Cope, 1881 being a notable exception, this ornamentation can be highly variable from individual to individual, along the tooth row, or even with tooth ontogeny. In *M. hoffmannii* the anterior marginal teeth tend to have two or three lateral facets, two being more common on the anterior dentary teeth and three being more common on the anterior maxillary teeth of the holotype. The medial facets are more numerous and less distinct, but there are usually at least five. The number of lateral facets increases posteriorly along the tooth row as the facets get narrower, and, perhaps more importantly, the lateral surface gets larger as the posterior carina shifts posteriorly.

3.b. Axial skeleton

Postcranial material of *Mosasaurus hoffmannii*, including vertebrae, is relatively rare, and the few specimens that do include postcranial elements are largely incomplete. No complete vertebral series was examined for this study, but representative vertebrae from the three major regions of the spinal column are described below. Atlas and axis elements are known from both European and North American specimens. Other cervical vertebrae are also known from both sides of the Atlantic Ocean, and two cervicals are found in the holotype. Five dorsal vertebrae, which appear to articulate, contribute to NHMM 006696, which also contains a terminal caudal. Owing to the incomplete nature of these various specimens, no vertebral counts are included in this study.

3.b.1. Atlas

Like all mosasaurids, the atlas of *Mosasaurus hoffmannii* is composed of four elements: the atlas intercentrum, the atlas centrum and the paired atlas neural arches. Anteriorly (Fig. 15a), the atlas neural arch is

a laterally bowed structure dominated by the antero-medial sub-rectangular articulation for the occipital condyle. The spinous process arches dorsomedially and is expanded and rugose distally. Because the spinous process is relatively short in *Mosasaurus hoffmannii*, it is unlikely that the two neural arches contacted each other on the midline, but the rugosity suggests a cartilaginous structure bridged the gap between the two neural arches. A short, blunt process protrudes from the ventrolateral corner of the condylar articulation. The condylar articulation is laterally convex, and the medial boarder is similarly concave. The dorsal border of the condylar articulation is roughly horizontal, but the ventral border angles dorsomedially. The anterior articular surface is also gently concave.

The neural arch extends posteriorly to form a bluntly tapered synapophyseal process (Fig. 15b). The articular facet for the axis is a vertically elliptical surface facing posteromedially. The posterior margin of the spinous process is indented by a shallow sulcus that terminates midway between the spinous and synapophyseal processes, approximately even with the posterodorsal corner of the articular body of the neural arch. This sulcus likely provided attachment surfaces for tendons (Russell, 1967).

Laterally, the atlas neural arch resembles an asymmetrical arrowhead because the ventral process is shorter than the spinous process (Fig. 15c). The anterior margins of the spinous and ventral processes are not confluent with the anterior surface of the condylar articulation but are posteriorly offset; this offset is greater between the condylar articulation and the ventral process with a notch formed between the two. The distal end of the spinous process bears a short crest that originates at the anterior corner, extends posteroventrally, but terminates at the mid-width of the spinous process.

The complexities of the articular body of the atlas neural arch are most evident in medial view (Fig. 15d). The articular body is medially offset from the surface formed by the confluent spinous and synapophyseal processes, roughly quadrilateral and bears four articular facets. Anterior-most is the vertical condylar articulation facet. Posterior to the condylar facet are the ventrally directed facet for the atlas intercentrum and, dorsal to that, the medially directed facet for the atlas centrum. A posteroventrally oriented ridge separates the facets for the two elements of the atlas centrum. In medial view, the facet for the atlas intercentrum is triangular with the anterior edge vertical and the ventral edge gently dorsally inclined. The facet for the atlas centrum is also sub-triangular, but the dorsal edge is concave. A posterodorsally oriented ridge separates the facet for the atlas centrum from the facet for the axis, which is oblong in medial view. The spinous process extends anterodorsally above the facet for the atlas centrum, and its distal termination is anteriorly expanded and vertically striated, probably for articulation with a cartilaginous structure. The synapophyseal process extends beyond the facet for the axis. The ventral process is borne on a confluent flange of bone and is

oriented ventral to the point where the facets for the atlas intercentrum, centrum and the axis converge near the ventral edge of the articular body.

In dorsal view (Fig. 15e) the sulcus along the posterior edge of the spinous process is distinct. The sulcus broadens slightly into a shallow pit at its ventral termination, approximately even with the posterodorsal corner of the articular body. A transverse ridge forms the posterior wall of this pit. Ventrally (Fig. 15f), the condylar articulation is seen to be gently concave. The articular facet for the atlas intercentrum is triangular from this view as well. The ventrolateral surface of the ventral process is rough and irregular, though this could partially be due to weathering and preservation.

The atlas centrum is rectangular anteriorly and posteriorly (Fig. 15g, h), but the anterior face is transversely convex and the posterior surface bears a vertical ridge that becomes narrower and steeper ventrally. Laterally, a sigmoidal ridge separates the inverted triangular facets that articulate with the atlas neural arch from the posteromedially sloping surfaces that articulate with the axis (Fig. 15i). In dorsal view, the atlas centrum is deeply bowed anteriorly and flat to shallowly convex posteriorly (Fig. 15j). In ventral view the atlas centrum is anteroposteriorly compressed and broadly triangular with the apex formed by the posterior ridge (Fig. 15k). In both anterior and posterior views the ventral edge of the atlas intercentrum is deeply bowed (Fig. 15l, m). The dorsal border is also convex, but the margin is not smooth: the dorsal margin is gently indented at the midline and pinched out at the lateral corners. The element is wedge-shaped laterally with a wide ventral surface and anterior and posterior faces that incline towards each other dorsally (Fig. 15n).

3.b.2. Axis

The anterior articular face of the axis (Fig. 16a) is sub-triangular with the apex ventral to, and recessed from, the rest of the broad articular surface. This recessed ventral area accepts the axis intercentrum. The centre of the anterior face articulates with the atlas centrum and is indented, with the indentation deepening ventrally into a broad triangular notch, to accept the posterior ridge of the atlas centrum. The lateral regions of the anterior face angle posterodorsally and articulate with the synapophyseal processes of the atlas neural arches. The base of the axis neural arch is broad, with each robust arch lamina rising dorsal to the lateral corners of the articulation for the atlas centrum. The neural canal is broadly triangular, but the anterior of the neural spine is damaged; therefore, the prezygapophyses are not preserved.

Posteriorly (Fig. 16b), the axis more closely resembles the subsequent cervical vertebrae. The condyle is round and approximately equal in height and width. The neural canal is tall and arched, and robust postzygapophyses project posterolaterally from the neural spine posterodorsal to the neural canal. Dorsoventrally compressed transverse processes project posterolaterally

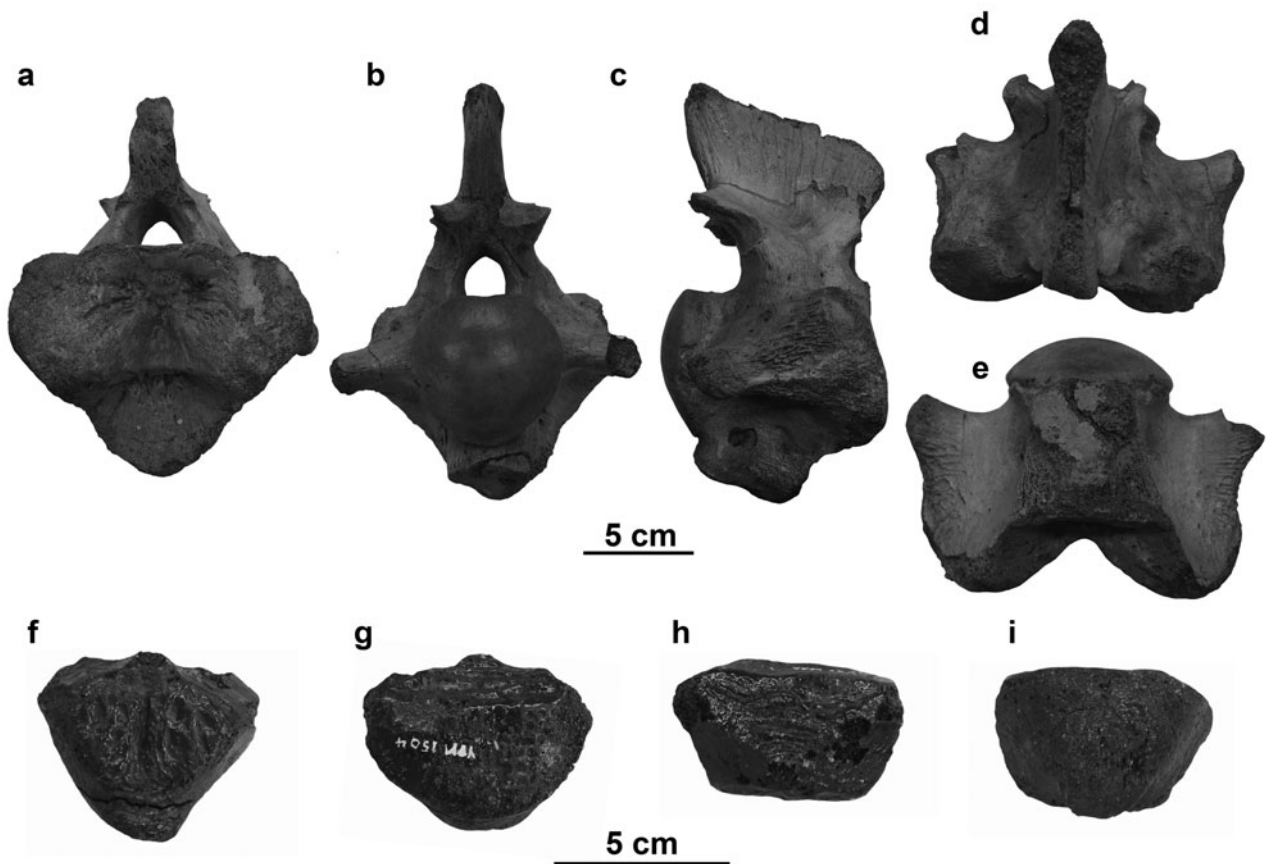


Figure 16. Axis of IRSNB R 26 in (a) anterior view, (b) posterior view, (c) lateral view (left lateral view shown, reflected for consistency), (d) dorsal view, and (e) ventral view. Axis intercentrum of YPM 1505 in (f) anterior view, (g) posterior view, (h) dorsal view, and (i) ventral view. Scale bars equal 5 cm.

around the condyle at mid-height. A robust hypapophysis descends from the ventral surface of the centrum posterior to the articular facet for the axis intercentrum.

The neural spine is distally expanded anteroposteriorly, even if it is incomplete dorsally, and tapers into the neural arch (Fig. 16c). The neural arch is not centred on the centrum but located on the anterior two-thirds of the element. The transverse processes are confluent with, and heavily buttressed to, the lateral extremities of the anterior articular surface. The posterodorsally facing articular facets for the atlas neural arch synapophyses are smoother and distinct from the rough lateral surfaces of the buttresses, which bear longitudinal ridges. The ventral hypapophysis angles posteroventrally and terminates approximately evenly with the condyle.

In dorsal view (Fig. 16d), the axis is widest posteriorly where the transverse processes flare laterally from the buttresses that join them to the lateral extremities of the anterior articular face and the posterolateral surfaces of the centrum. The lateral extremities of the articular surface are convex anteriorly around the median concavity for receiving the atlas centrum. The neural spine likely would have been longer than the ventral length of the centrum when it was complete.

In ventral view, the hypapophysis arises directly from the posterior of the facet for the axis intercentrum

(Fig. 16e). The hypapophysis is weathered, obscuring the outline of the articulation to the peduncle. The axis centrum is slightly constricted between the condyle and the posteriorly concave transverse processes, but this constricted region is quite short. The lateral margin of the buttress between the transverse processes and the lateral extremities of the anterior face are sinuous, and the depth of the median concavity for the atlas centrum is most evident in ventral view.

The axis also has a separate intercentrum that articulates to the ventral portion of the anterior articular face (Fig. 16f–i). The axis intercentrum is a sub-triangular block of bone that tapers posteriorly (Fig. 16i). Both the anterior and posterior articular faces are quite rugose, likely for articulation with cartilage, but the posterior surface is also indented dorsally, forming a horizontal shelf (Fig. 16f, g). There is a low anteroposteriorly oriented ridge on the dorsal surface of the axis intercentrum, and the entire element tapers ventrally (Fig. 16h).

3.b.3. Cervical vertebrae

Two cervical vertebrae, identifiable by the hypapophyses visible on the ventral surfaces of the centra, are

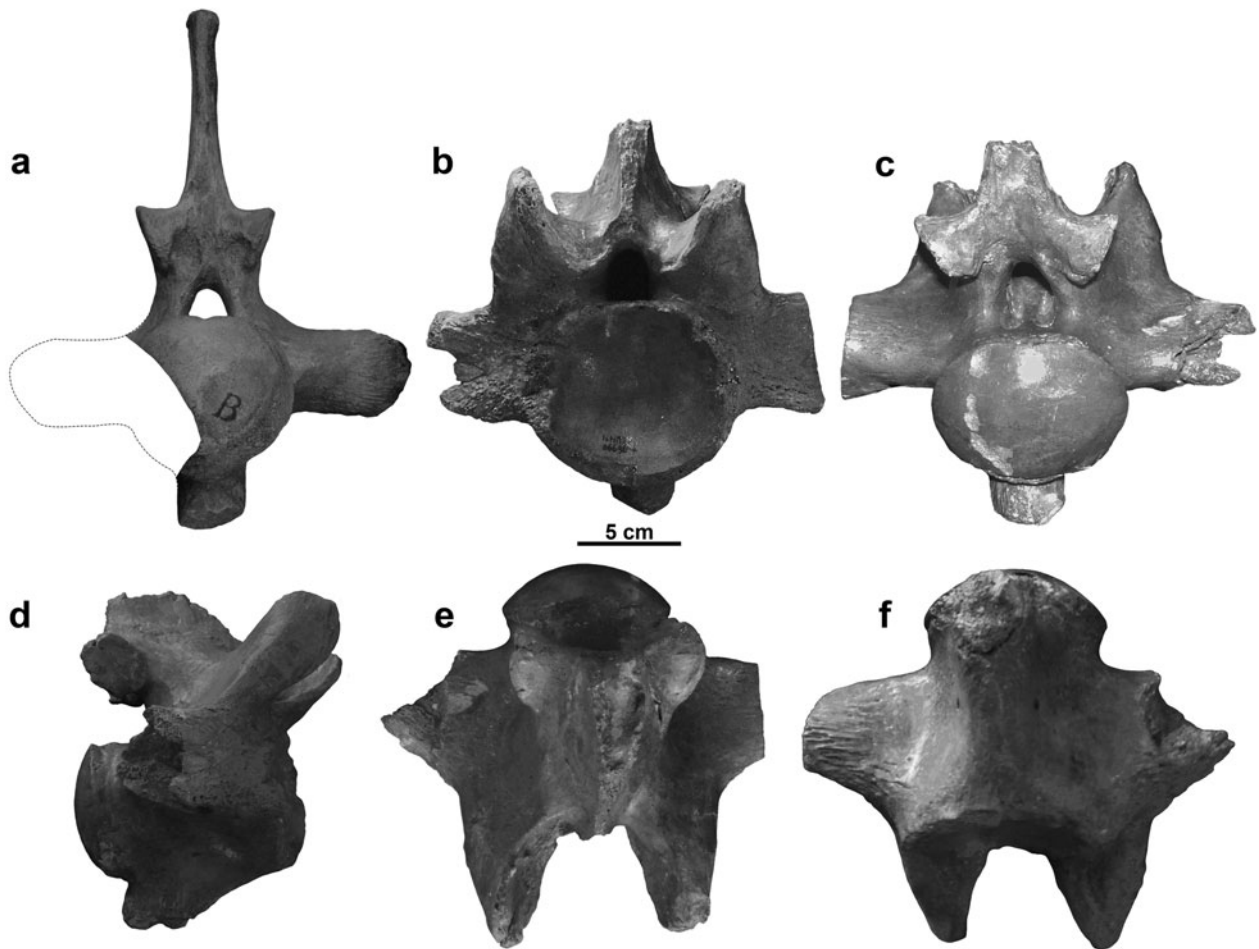


Figure 17. Cervical vertebrae. (a) MNHN AC 9648 in posterior view. (b–f) NHMM 006696 in (b) anterior view, (c) posterior view, (d) right lateral view, (e) dorsal view, and (f) ventral view. Note: letters visible on the fossil have been painted on the specimen and bear no association with the labelling system of this study. Scale bar equals 5 cm.

preserved with the skull of MNHN AC 9648, but they are embedded in the block and partially concealed by the mandibles (Fig. 1). The length of these cervical centra exceeds the height and the width, and the condyles are quite circular because the width and height are nearly equal. The cervical vertebrae each bear a robust, posteriorly directed hypapophysis on the posterior half of the ventral surface of the centrum (Fig. 17a). The transverse processes extend laterally from the mid-length of the lateral surface of the centrum, slightly above mid-height. A buttress extends posteriorly from the transverse processes but terminates anterior to the condyle. The neural arches arise further anterior on the centrum and must bear both pre- and postzygapophyses and zygosphenes/zygantra. Even though the prezygapophyses and zygosphenes are embedded in the block, the postzygapophyses and zygantra suggest the articulating anterior structures would be present. The articular facets of the postzygapophyses, which are oriented at a 30° angle from the neural spine, are oval in lateral view. Posteriorly, the zygantra are a pair of pits at the base of the neural spine medial to the postzygapophyses. The neural spine is tall and blunt at its distal termination.

Along the cervical series there is a great deal of variation in the morphology of the prezygapophyses, as is seen when comparing vertebrae MNHN AC 9648 and NHMM 006696 (Fig. 17). There is greater confluence between the prezygapophyses and the transverse processes in the NHMM 006696 cervical vertebra than is seen in the cervicals of MNHN AC 9648, so these vertebrae presumably came from different positions along the cervical series. The postzygapophyses are more offset from the neural spine in NHMM 006696 and the transverse processes appear broader owing to the buttress between the prezygapophyses and the transverse processes.

The cotyle of NHMM 006696 is concave and the rim is not depressed dorsally at the floor of the neural canal (Fig. 17b). The posterior condyle is slightly wider than it is tall and faintly depressed dorsally for the floor of the neural canal, unlike the uninterrupted rim of the cotyle (Fig. 17c). The condyle is more deeply rounded in dorsal and ventral views than it is in lateral view (Fig. 17d–f).

The transverse processes extend horizontally from the lateral faces of the centrum oriented slightly dorsal to the mid-height of the centrum in anterior view

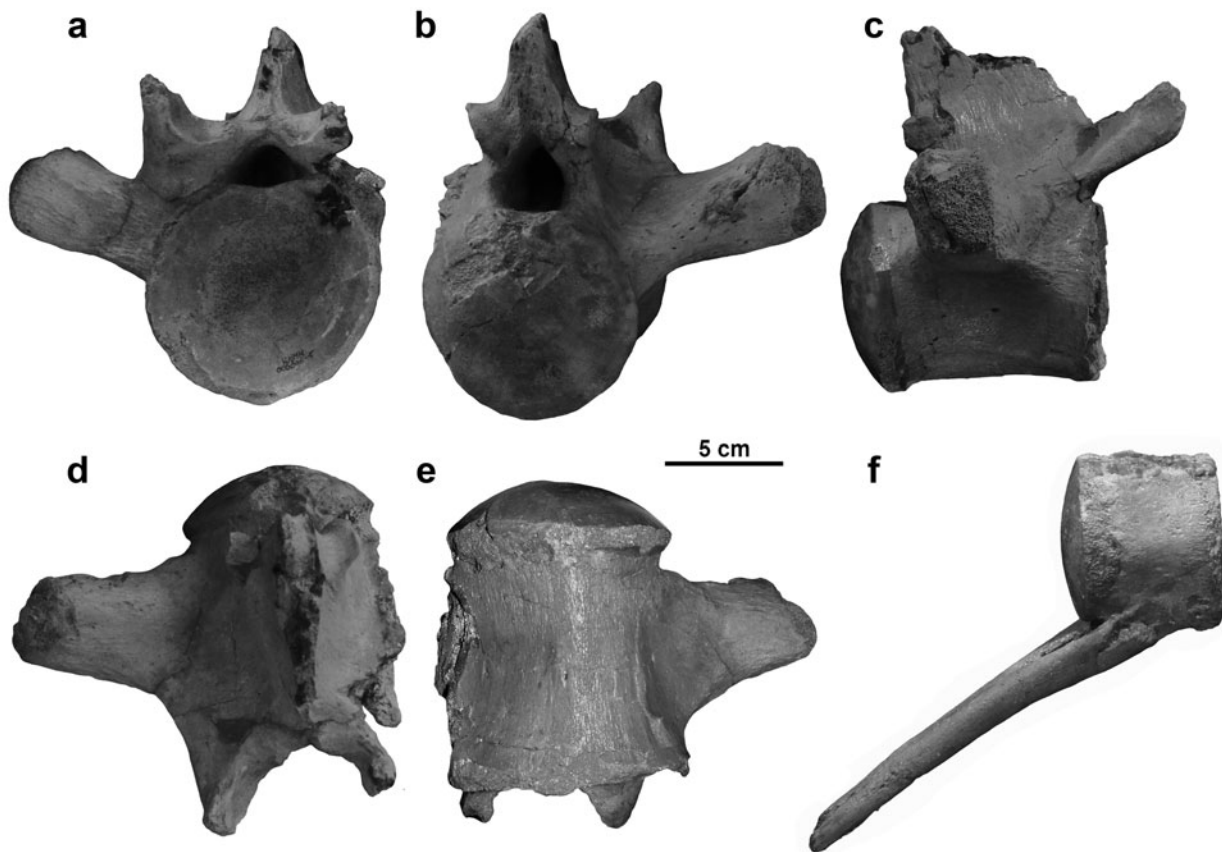


Figure 18. Dorsal (a–e) and caudal (f) vertebrae of NHMM 006696 in (a) anterior view, (b) posterior view, (c) right lateral view, (d) dorsal view, (e) ventral view, and (f) right lateral view. Scale bar equals 5 cm.

(Fig. 17b), but in lateral view (Fig. 17d), it is clear that the transverse processes of NHMM 006696 are actually oriented posterolaterally with the anterior face being nearly vertical and the posterior side being deeply convex.

The dorsal surfaces of the transverse processes merge smoothly into the prezygapophyses (Fig. 17c, e). The prezygapophyses are robustly supported; the distance between the dorsomedially oriented articular facets themselves is narrower than the width of the centrum, but the lateral edges of the prezygapophyses are wider than the width of the articular cotyle (Fig. 17b). The space between the prezygapophyses describes a broad U-shape (Fig. 17e). The postzygapophyses do not extend further caudally than the condyle of the centrum, but the prezygapophyses project considerably cranially beyond the cotyle of the centrum (Fig. 17d). The articular facets of the postzygapophyses are broadly oval and inclined posterodorsally.

Posteriorly (Fig. 17c), the neural canal of NHMM 006696 is tall and arched with slightly convex sides and a faint ridge extending along the length of its floor. Medial to the dorsolaterally slanted postzygapophyses are two shallow zygantra at the base of the neural spine, suggesting that there would have been small zygosphenes in life. The neural spine is broken just dorsal to the zygapophyses, but it appears that the anterior edge might have been slanted posteriorly while the posterior edge was nearly vertical.

The robust hypapophysis is smoothly buttressed to the anterior edge of the ventral surface of the centrum, and posteriorly it terminates before the posterior edge of the centrum with a nearly vertical face (Fig. 17d, f). Ventrally (Fig. 17f), there is a pair of small foramina on either side of the keel formed by the anterior buttress of the hypapophysis. The articular surface of the hypapophysis is sub-triangular and rugose.

3.b.4. Dorsal vertebrae

Like the cervical centra, the dorsal vertebral centra of NHMM 006696 are longer than they are tall or wide, and slightly wider than they are tall (Fig. 18). The articular face is sub-circular in anterior view and slightly depressed dorsally for the floor of the neural canal, which is broadly triangular (Fig. 18a). Posteriorly (Fig. 18b), the articular condyle is convex and subequal in width and height. The neural canal forms a shallow depression dorsally on the centrum and exits the neural arch in a triangular opening that is taller than wide. In lateral view (Fig. 18c), the ventral surface of the centrum is slightly concave between the articular faces. The ventral surface of the centrum forms a keel that extends its entire length (Fig. 18e). Additionally the centra become shortened, but owing to the incomplete state of the dorsal series, the position of this transition is unknown.

As is typical of mosasaurines, the neural arches and spines are oriented anteriorly on the centra. Therefore, the prezygapophyses project considerably beyond the anterior articular face of the centrum to contact the sub-circular postzygapophyses on the posterolateral base of the preceding neural spine (Fig. 18c). It appears that the length of the anterior zygapophyses becomes less exaggerated posteriorly as the neural arches and transverse processes become more centred on the centra. The prezygapophyses are widely spaced, with their lateral surfaces being approximately even with the lateral faces of the centrum, and therefore the base of the neural arch is approximately as wide as the centrum (Fig. 18a). Like in the cervical vertebrae, the space between the prezygapophyses describes a broad U-shape (Fig. 18d).

On the dorsal vertebrae, the postzygapophyses are considerably reduced in comparison to the cervical vertebrae, and they are not as offset from the neural spine either posteriorly or laterally (Fig. 18b–d). Unlike the cervical vertebrae, where the long axis of the broadly oval postzygapophyseal facets is oriented steeply posterodorsally, the long axis of the smaller, sub-circular zygapophyseal facets of the dorsal vertebrae is oriented shallowly anterodorsally.

The transverse processes are robust, oriented above the dorsoventral midline of the centrum, and extend at a dorsolateral angle from the base of the neural arch (Fig. 18a, b). The transverse processes have a slight posterior angle and a strong anterior buttress that extends to the anterior articular surface (Fig. 18c). The dorsal edge of the buttress is confluent with the lateral buttress of the prezygapophyses. The transverse processes are buttressed posteriorly, but the buttresses are not as strong as the anterior buttresses and do not reach the condyle. The rib head articular facets of the transverse processes are variable in shape, but tend to be slightly compressed anteroposteriorly, broader dorsally and variably pinched ventrally, giving the transverse processes an inverse sub-triangular cross-section.

No well-preserved zygosphenes were observed, but small bumps between the prezygapophyses and the neural spine could be what remains of these structures (Fig. 18a). Shallow concavities at the base of the neural spine are likely reduced zygantra (Fig. 18b).

3.b.5. Caudal vertebrae

The only caudal vertebra preserved in NHMM 006696 is a terminal caudal of unknown position (Fig. 18f). The terminal caudal vertebrae are proportionately the shortest of the vertebrae in derived mosasaurs, and at this point in the caudal series the width and height are subequal. The degree of concavity/convexity of the condyles/cotyles is also reduced. There are no transverse processes, and, owing to the state of preservation, the morphology of the neural arch and spine is unknown. However, the chevrons are well preserved. The proximal end of the chevron is fused with the

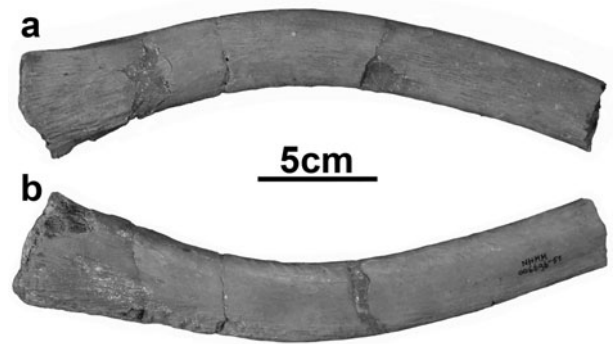


Figure 19. Rib of NHMM 006696 in (a) left anterior view and (b) left posterior view. Scale bar equals 5 cm.

ventrolateral edges of the centrum at the midpoint of the centrum's length. The two halves of the chevron extend posteroventrally and medially to fuse along the midline. The chevrons are more than twice as long as the centrum.

3.b.6. Dorsal ribs

The ribs of NHMM 006696 are anteroposteriorly compressed, with oval articular facets. Proximally, the ribs are straight, but they bow into a gentle curve (Fig. 19a, b). Some ribs appear to have fossae or broad grooves where the degree of curvature is the greatest, but whether this is a true morphologic feature or the result of taphonomy is unclear.

3.c. Appendicular skeleton

Appendicular material is quite sparse for *Mosasaurus hoffmannii*. No articulated pectoral or pelvic girdles or limbs were observed. The girdles and propodial limb elements will be described below based on various referred specimens from Europe. Appendicular material is even rarer from North America, though whether this is the result of the poor preservation of strata like the New Jersey greensands or from collection bias is uncertain.

3.c.1. Scapula

The scapula should be a large, fan-shaped structure, subequal in size to the coracoid, but no complete element is known for this species. The incomplete right scapula of IRSNB R 26 does preserve the articular head and the characters thereon (Fig. 20). The head of the scapula is offset from the flat plate of the scapular blade by approximately 45°. A broad ridge separates the two articular facets on the scapular head (Fig. 20a). Facing posterolaterally is the facet that contributes to the glenoid fossa for the head of the humerus. This facet is broadly concave laterally, but where the facet crosses the axis formed by the scapular body it curves into a medial convexity. The outline of this facet is partially obscured by weathering to the medial side of

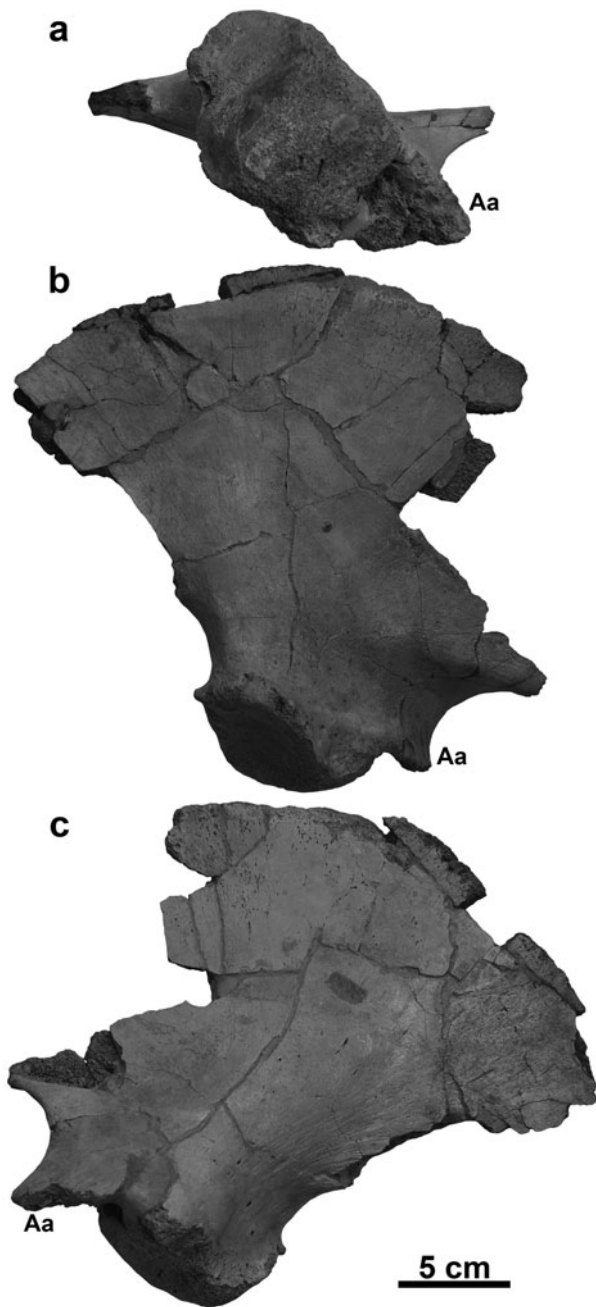


Figure 20. Scapula of IRSNB R 26 in (a) right proximal view (b) right lateral view, and (c) right internal view. Abbreviation: Aa – anterior accessory articulation. Scale bar equals 5 cm.

the scapular head, but it appears to be U-shaped. The articular facet for the coracoid is sub-quadrilateral and faces anteromedially. The surface of the facet for the coracoid is flatter than that for the humerus, but the remnants of the surficial layer of bone indicate that it would have been more rugose. An additional process, descending from the anterior edge of the scapular neck appears to have served as an accessory articulation to the coracoid. This process is dorsally offset from the scapular head laterally, and projects anteriorly, but it is more confluent with both the head and blade of the scapula medially. This accessory process is also seen

in *M. lemonnieri* and *M. missouriensis*, but it does not appear to be unique to *Mosasaurus*. Russell (1967) illustrated similar expansions on the necks of the pectoral girdle elements for both *Clidastes liodontus* and *Platycarpus*, though it is quite reduced in the latter taxon. However, because this anterior accessory articulation is not as well developed in those taxa, the structure was not described extensively.

The development of the anterior accessory process means that while the scapular neck is constricted, it is unusually long anteroposteriorly. In lateral view (Fig. 20b), the anterior of the scapular neck is even with the plane formed by the long axis of the scapular head and is offset from the blade of the scapula. Anteriorly a broad, C-shaped canal forms between the anterior accessory process and a ridge that marks the ventral edge of the scapular blade. This ridge likely continued anteriorly, and its posterior termination is dorsal to the ridge that separates the glenoid and coracoid articular facets on the scapular head. Internally, the neck of the scapula is bowed by the medial termination of the coracoid facet (Fig. 20c). The scapular blade is thickest dorsal to the head of the scapula. The blade of the scapula is broken both anteriorly and posteriorly, so the degree of curvature of the dorsal margin, how far the scapular blade extended anteriorly or posteriorly, and any asymmetries of that extent are unknown.

3.c.2. Coracoid

An incomplete left coracoid is known for NHMM 006696, but owing to the poor state of preservation some characters of this element, including the morphology of the margin and the articular facets, remain uncertain (Fig. 21). The robustly supported articular facets are directed posterolaterally, and the thinning, dished blade of the coracoid extends medially in an extending fan. The facets for the scapula and the humerus are borne on a broad elliptical fossa with a faint vertical crest separating the anterodorsal scapular facet from the larger glenoid fossa. However, taphonomic fracturing and weathering of the coracoid neck obscures these features. Medial to the coracoid head, the posterior margin of the element is concave, forming a neck that separates the glenoid fossa from the body of the coracoid, but anteriorly the neck is not waisted (Fig. 21a). Instead of forming a concave margin to further constrict the neck of the coracoid, a straight-margined flange originates anterior to the coracoid foramen and extends laterally towards, but does not quite reach, the articular facets. The surface of this flange is slightly rugose and is reminiscent of the interdigitating structure described by Russell (1967) for *Clidastes* and *Mosasaurus conodon* and in *M. hoffmannii* it appears that the structure would have articulated with the anterior accessory process of the scapula.

Medial to the neck, the coracoid thins considerably as it expands into a broad fan. A thicker bar extends

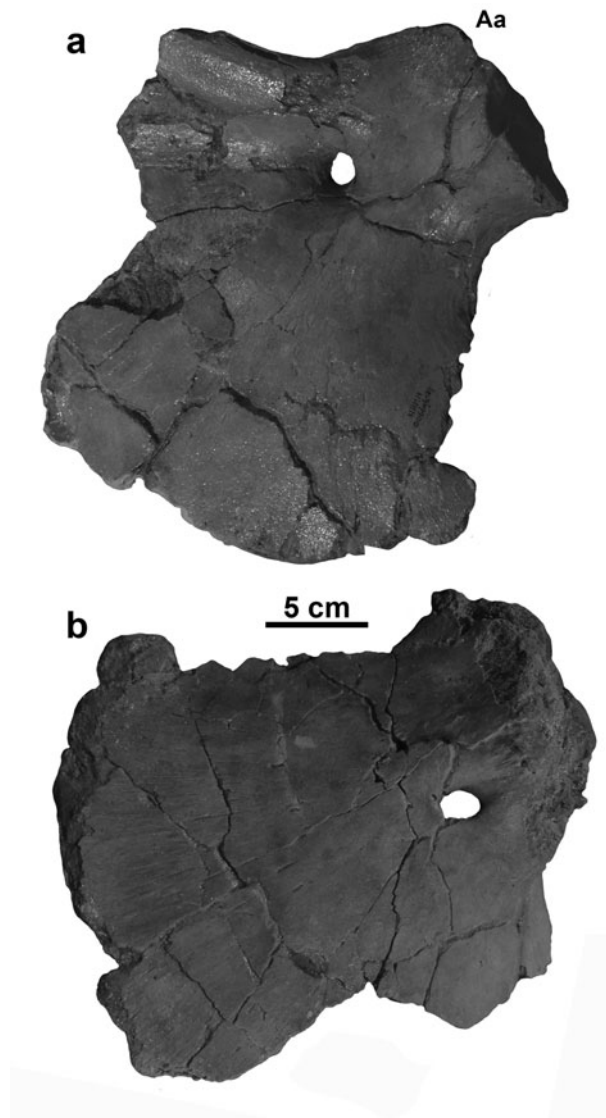


Figure 21. Coracoid of NHMM 006696 in (a) left ventral view and (b) left internal view. Abbreviation: Aa – anterior accessory articulation. Scale bar equals 5 cm.

anteromedially from the head anterior to the foramen, and the coracoid is thinnest medial to the foramen. This anteromedial region of the coracoid is least complete, so the morphology of the border is unknown, but the angles of the preserved margins suggest that the coracoid was symmetrical anteroposteriorly, or that the posterior margin was slightly longer. Internally (Fig. 21b), the coracoid appears to be evenly convex. The poor state of preservation of the head and margin in this view prevents observation of other diagnostic characters.

3.c.3. Humerus

The humerus of *Mosasaurus hoffmannii* typifies the mosasaurine condition being long for its height and complexly three-dimensional (Fig. 22), differing from the more elongated, less-well-ossified humeri of *Platycarpus* or *Tylosaurus* (Russell, 1967). Even the humeri

of *Clidastes* and *Prognathodon* are not as robust as that of *Mosasaurus* (Russell, 1967; Konishi *et al.* 2011). Unfortunately, no complete humerus is known for *M. hoffmannii*, and the humerus of IRSNB R 26 is the most complete though it lacks much of the postaxial half of the element. Sufficient portions of the proximal and preaxial bone are preserved to allow for the observation of distinguishing characters.

In medial view or lateral view, a complete humerus of *Mosasaurus hoffmannii* would likely have been as long or longer anteroposteriorly than it is tall (Fig. 22a). Proximally, the glenoid facet and the pectoral crest contribute to the proximal width of the humerus, and these confluent structures form a dorsally bowed surface (Fig. 22b). Proximally (Fig. 22d), the glenoid fossa is a large, oblong facet that is slightly concave medially but convex laterally where it merges with the laterally projecting pectoral crest. The post-glenoid process projects posterodorsally from the postaxial side of the glenoid fossa (Fig. 22a–d). This structure is robust, separate from the glenoid articular fossa, bluntly rounded, and has parallel sides (Fig. 22c).

The humerus is constricted slightly dorsal to the mid-height of the bone, and this constriction forms a U-shaped embayment in the preaxial surface of the element. Distal to the constriction the ectepicondyle extends further anteriorly than the glenoid facet. The ectepicondyle is bluntly tapered, and its distal surface is the straight articular facet for the radius, which faces anterodistally. In distal view (Fig. 22e), the articular facet for the radius is flat and ovoid in outline, being slightly more convex medially than laterally and narrowest at the anterior termination of the ectepicondyle. The radial facet appears to be separated from the ulnar facet by a medial notch, as is seen in other mosasaurines such as *Plotosaurus* (Russell, 1967).

Posterior to the preaxial constriction, the pectoral crest arises from the medial surface of the humerus. It is confluent with the medial extent of the glenoid facet, where it is most prominent, and tapers into the surface of the element distally (Fig. 22a, b). The distal termination of the pectoral crest is even with the ectepicondyle. The entepicondyle is not preserved.

The lateral view of the humerus (Fig. 22c) is similar in outline to the medial side, but the lateral surface is flatter without such prominent elaborations for muscle attachments, though there is a rugose patch around the distal-most portion of the element. The surface of the humerus proximal to the apex formed between the radial and ulnar facets is also slightly roughened and would have been the attachment site for the latissimus dorsi muscle. The glenoid facet does extend slightly laterally beyond the plane of the element. Between the glenoid facet and the distal rugosities a pair of foramina are situated in a groove that angles anterodistally. For the moment it is uncertain whether this structure is at all comparable with the ectepicondylar groove seen above the radial facet in platycarpines and tylosaurines that

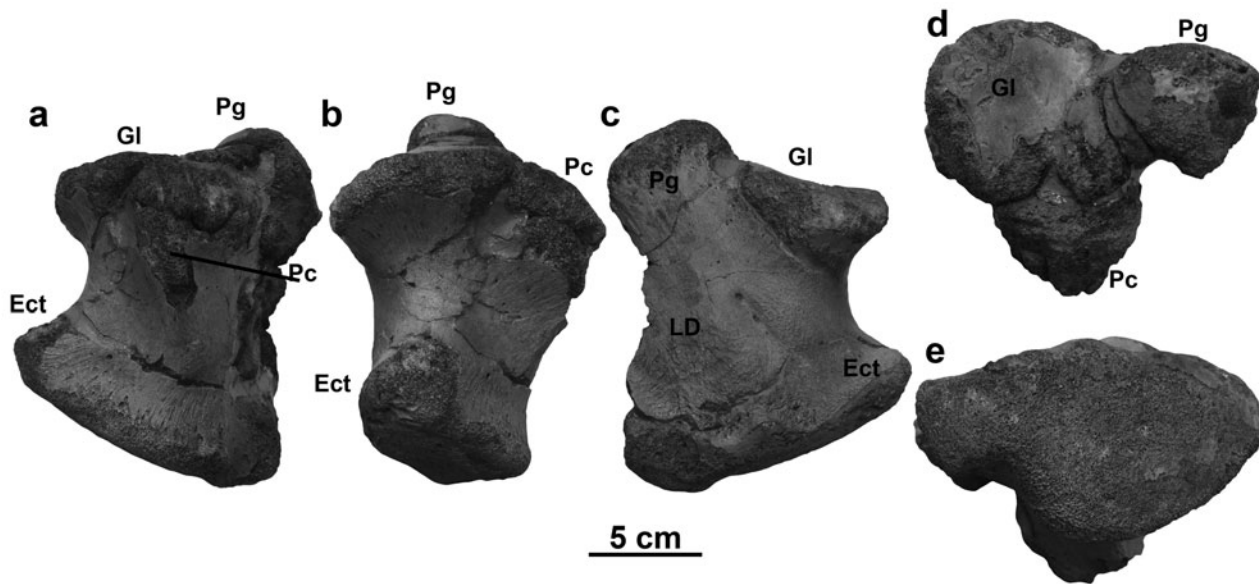


Figure 22. Humerus of IRSNB R 26 in (a) right medial view, (b) right preaxial view, (c) right lateral view, (d) right proximal view, and (e) right distal view. Abbreviations: Ect – ectepicondyle; Gl – glenoid fossa; LD – attachment site for latissimus dorsi muscle; Pc – pectoral crest; Pg – postglenoid process. Scale bar equals 5 cm.

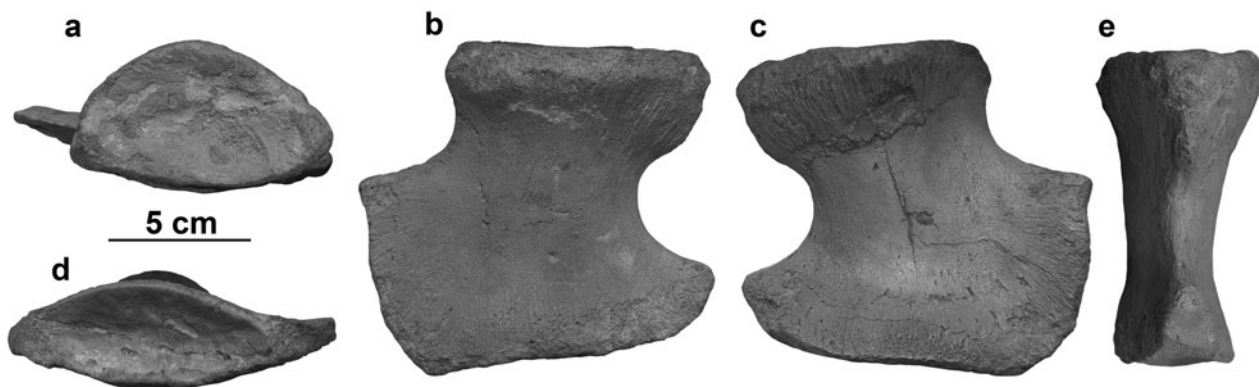


Figure 23. Radius of IRSNB R 299 in (a) left proximal view, (b) left lateral view, (c) left medial view, (d) left distal view, and (e) left postaxial view. Scale bar equals 5 cm.

Russell (1967) interpreted as conveying the radial nerve. An ectepicondylar groove has not yet been reported from a mosasaurine mosasaur, and additional research and observation of other mosasaurines would be necessary to determine the possible homology of these structures.

3.c.4. Radius

The radius is robust and distally expanded, as is typical in mosasaurines (Fig. 23). The proximal articular facet of the radius is D-shaped with the bowed side medial and the flatter surface lateral (Fig. 23a). Distal to the articular head, the radius is asymmetrically waisted, with the constriction of the preaxial margin located more proximally than the constriction of the postaxial margin (Fig. 23b, c). The concavity to the preaxial margin is shallower and broader than that to the postaxial

margin, which is more deeply U-shaped. Distal to the constriction of the radial shaft, the element expands and thins anteriorly and posteriorly. The distal articulation for the radiale is approximately parallel to the proximal articular surface but much thinner and lenticular in outline (Fig. 23d). As is typical of mosasaurines, a wing of bone extends anteriorly forming an anterodistal flange. In IRSNB R 299 the truncation of this flange forms a nearly right angle between the preaxial margin and the distal articular facet, but in life the preaxial margin was likely curved. Significant distal expansion of the radius is seen in most groups of derived mosasaurs except *Tylosaurus*, but the distal end of the radius of *M. hoffmannii* most closely resembles that of *Clidastes*. However, the proximal end of the radius in *Clidastes* is narrower (Russell, 1967). Postaxial to the articular facet for the radiale is a secondary articular facet oriented at an obtuse angle to the main distal articular surface

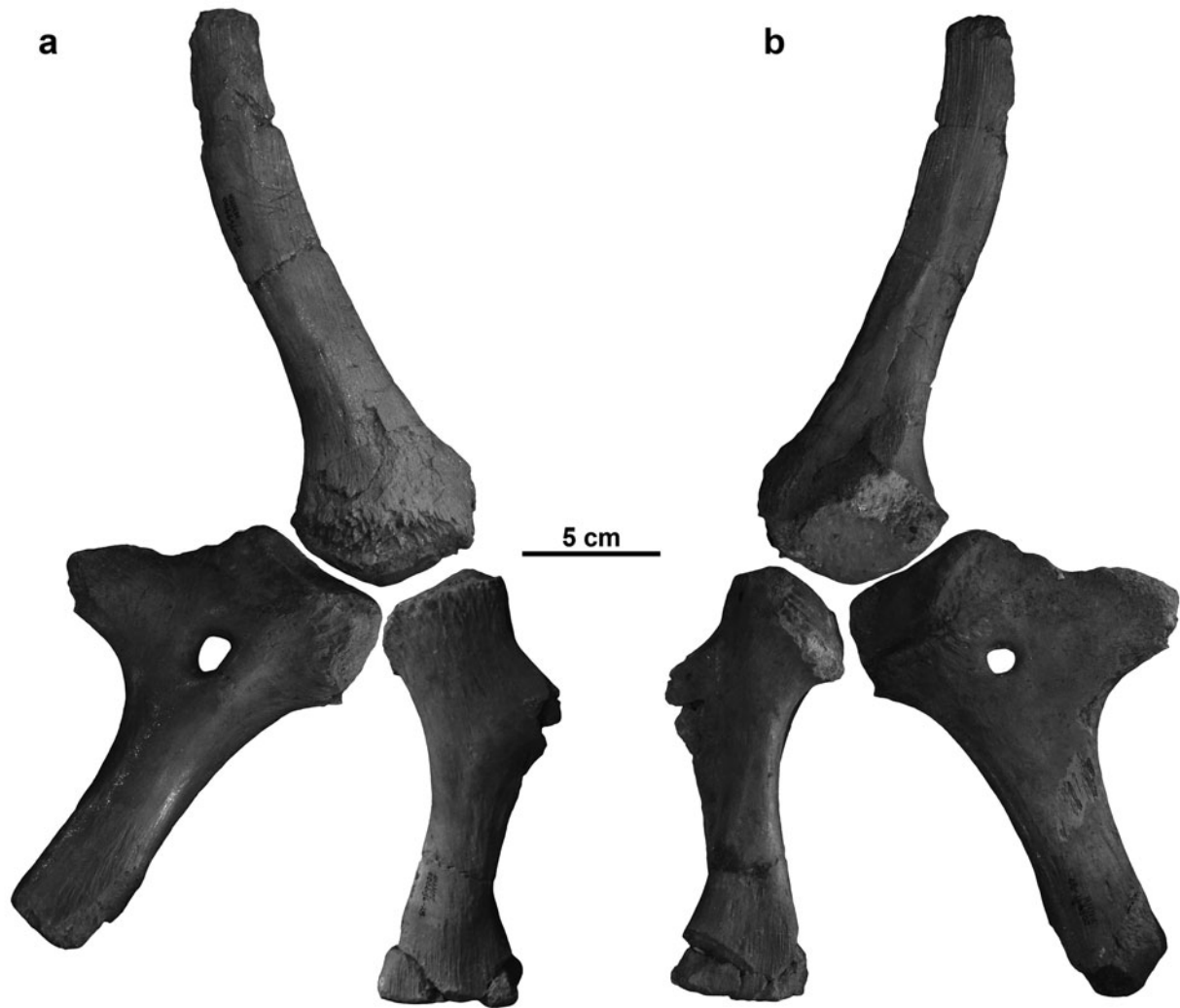


Figure 24. Pelvic girdle reconstructions of NHMM 006696, left pubis reflected to articulate with right ilium and ischium in (a) right medial view and (b) right lateral view. Scale bar equals 5 cm.

(Fig. 23e). This smaller facet is triangular in postaxial view and most likely articulated with the intermedium.

3.c.5. Ilium

The ilium of NHMM 006696 is the longest of the three pelvic bones (Fig. 24). As is the case for all fully marine, hydropelvic mosasaurs (Caldwell & Palci, 2007), the ilium is comprised of a slender dorsal shaft that broadens into a ventral head bearing the articular facets for the pubis, ischium and femur. The shaft is compressed and blade-like. Proximal to the acetabulum the ilium angles slightly anteriorly, but the distal end extends dorsally, giving the anterior border of the element a faintly recurved outline. The posterior border of the shaft is more nearly straight. The head is the most robust region of the element. Medially, the head of the ilium is rugose dorsal to the articular facets (Fig. 24a), which are borne laterally and ventrally (Fig. 24b). The facet for the pubis is ventral, that for the ischium is posteroventral, and the facet that contributes to the acetabulum is lateral and dorsally convex (Fig. 24).

3.c.6. Pubis

The pubis and the ischium of NHMM 006696 are subequal in length with the pubis being slightly longer and more robust than the ischium (Fig. 24). The shaft of the pubis is sub-circular to sub-triangular in cross-section and straight. The distal end of the shaft is striated or rugose on all sides; these structures are presumably the scars from muscle attachments. The anteroproximal edge of the shaft pinches out into a pubic tubercle or process, which is large and anteriorly directed. The edges of the process are straight and nearly parallel, but poor preservation of its distal end makes it unclear whether the termination of the process would have been triangular, as in *Mosasaurus conodon*, or rectangular, as in *Clidastes* (Russell, 1967). The pubic tubercle of *Prognathodon overtoni* is more gracile than that of *M. hoffmannii* (Konishi *et al.* 2011). The obturator foramen is wider and oval internally (Fig. 24a) and constricts as it passes through the pubis to exit as a small, sub-circular opening anterior to the ridge that extends along the external surface of the shaft from the acetabulum to its distal end (Fig. 24b). The obturator

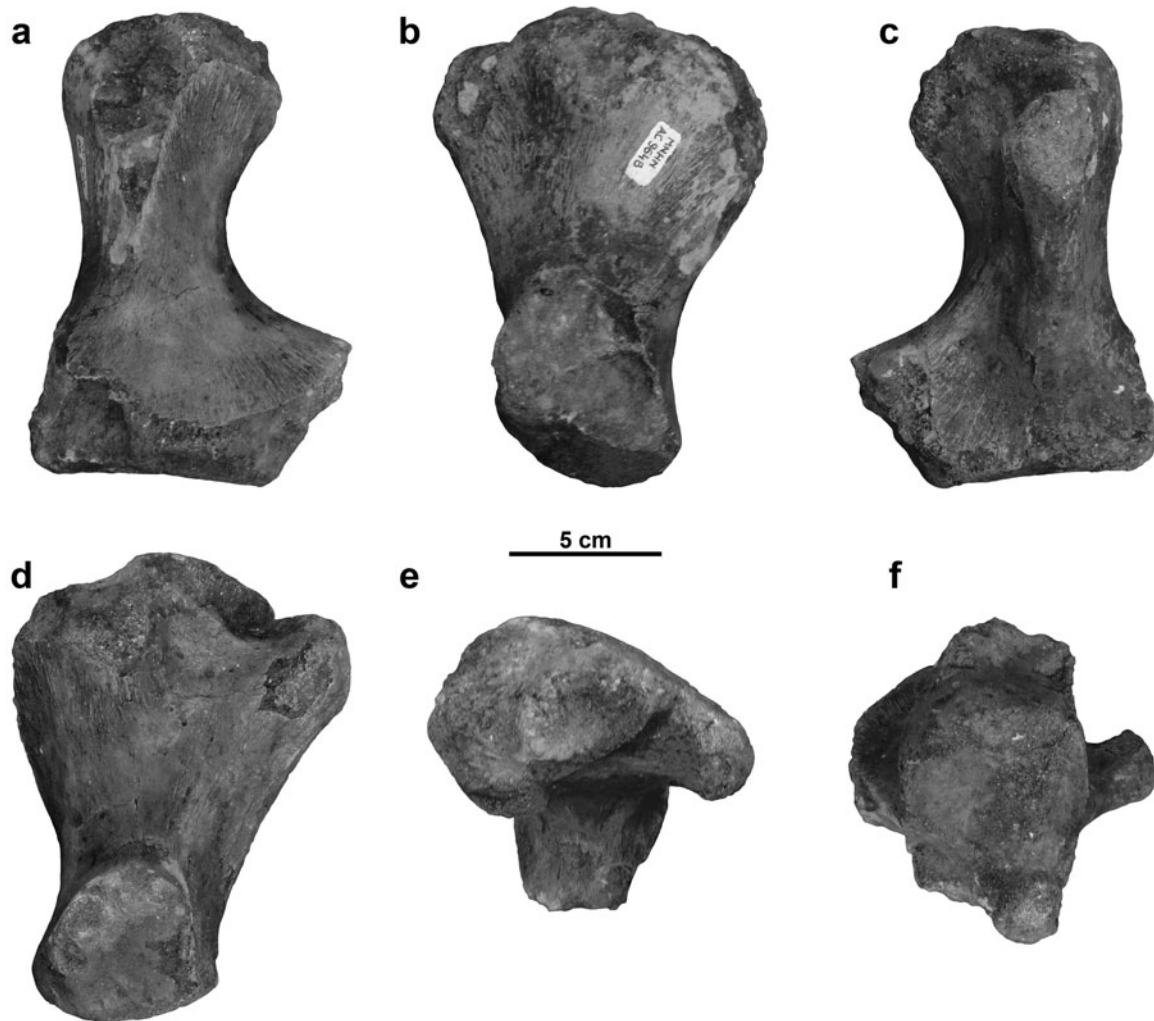


Figure 25. Left femur of MNHN AC 9648 in (a) lateral view, (b) preaxial view, (c) medial view, (d) postaxial view, (e) proximal view, and (f) distal view. Scale bar equals 5 cm.

foramen pierces the concavity between that ridge and the dished pubic process. The robust pubic head bears articular facets posteriorly for the ischium, posterodorsally for the ilium and laterally for the acetabulum. The facets for the ilium and the acetabulum are each concave.

3.c.7. Ischium

The head of the ischium of NHMM 006696 also bears three articular facets (Fig. 24b). Those for the ilium and pubis are flat to concave, and the facet that contributes to the acetabulum is convex. Internally, the surface of the anteroposteriorly expanded medial end of the shaft is striated where it would articulate with its counterpart on the midline, and the surface around the head is rugosely striated (Fig. 24a). There is a shallow fossa along the posterior edge of the middle of the bone, medial to the ischiadic process. This process arises from the posterodorsal border of the shaft slightly medial to the head. There is little constriction of a neck between the ischiadic process and the head of the is-

chium, with the posterior border being only slightly concave between the two. The borders of the shaft are more distinctly concave both posteriorly and anteriorly, and the anterior curvature of the bone is created by the anterolateral projection of the ischiadic head. Externally (Fig. 24b), the medial end of the ischium is striated, though the striations are shallower than those on the internal surface. The constriction of the shaft is more distinct in this view because the flange of the ischiadic process is offset from the shaft.

3.c.8. Femur

The left femur of MNHN AC 9648 is more weathered than the cranial elements (assuming it came from the same individual), and some of the features are obscured (Fig. 25). The articular surfaces for the acetabulum and the tibia and fibula are each expanded, but the axes of expansion are oriented at nearly right angles to each other. Between the condyles, the shaft of the femur is constricted, particularly in medial and lateral views. The distal end of the femur forms two distinct facets.

The larger facet is slightly longer than it is tall and accepts the tibia, and the smaller facet is laterally concave for the articulation with the fibula.

The lateral aspect of the femur (Fig. 25a) bears a crest that originates proximally from the femoral head and tapers to terminate at about the midpoint of the shaft. In this view, the preaxial surface of the bone is gently concave, and the postaxial edge is deeply concave, giving the trailing edge a broadly U-shaped outline. The distal end of the femur is the more expanded in this orientation for the articular facets of the tibia and fibula.

In preaxial view (Fig. 25b) the proximal end of the femur is fan-shaped, and the tapered region of the shaft appears very short. The fan-shaped proximal expansion is formed by the rounded, oval femoral head (Fig. 25e), which is confluent with the lateral crest, and the robust internal trochanter. The internal trochanter, positioned proximomedially on the shaft (Fig. 25b–e), does not extend as far proximally as the femoral head, and it is separated from the latter structure by a broad sulcus (Fig. 25d). A buttress supporting the internal trochanter extends distally about halfway along the shaft (Fig. 25c).

The distal articular facets are oriented approximately perpendicular to the long axis of the femoral head. The tibial facet is the larger of the two, and it is nearly perpendicular to the long axis of the femoral shaft. This facet would likely have been approximately rectangular. The fibular facet projects postaxially from the distal end of the bone, and the outline of the facet is a reflected D-shape. The fibular facet is more concave than that for the tibia (Fig. 25f). In lateral and medial views (Fig. 25a, c), the tibial and fibular facets meet in a slightly obtuse angle.

As with all the limb elements, the femur of *M. hoffmannii* differs greatly from those of other genera of mosasaurs. The femora of *Clidastes*, *Platecarpus* and *Tylosaurus* are all more elongated than in *Mosasaurus* (Russell, 1967). The femur of *Prognathodon overtoni* has many similar features, including a rounded femoral head, a robust internal trochanter and comparable distal articular facets, but even in *Prognathodon* the femur is more elongate and gracile (Konishi *et al.* 2011).

3.c.9. Tibia

The tibia of NHMM 006696 is approximately as long as it is tall (likely it would have been longer than tall if complete), and bears a thin, dished convex flange on its anterior edge (Fig. 26). Some degree of anterior expansion is exhibited by the tibiae of *Prognathodon* and *Tylosaurus* (Russell, 1967; Konishi *et al.* 2011), but that expansion is greater in *M. hoffmannii*. The main shaft and posterior edge are considerably thicker, and the posterior edge is deeply concave (Fig. 26a, b). The proximal articular facet for the femur is concave and ovoid, with the anterior end being narrower than the posterior end (Fig. 26c). The distal end bears two articular facets at a 120° degree angle to each other

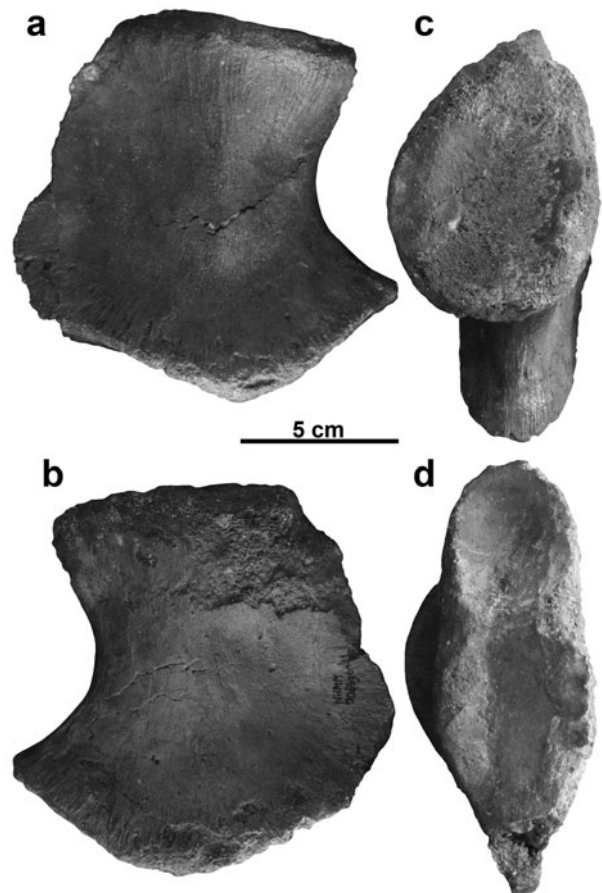


Figure 26. Left tibia of NHMM 006696 in (a) lateral view, (b) medial view, (c) proximal view, and (d) distal view. Scale bar equals 5 cm.

(Fig. 26d). The anterior facet for the first metatarsal is slightly deeper mediolaterally and teardrop shaped, and the posterior facet for the astragalus is shorter (both dorsoventrally and anteroposteriorly) and more deeply concave.

4. Discussion

4.a. Taxonomic history of *Mosasaurus*

Since 1822 approximately 50 species have been erected and assigned to the genus *Mosasaurus*. Several of these are junior synonyms for other species (there are at least four junior synonyms of *M. maximus*, which itself is a junior synonym of *M. hoffmannii* (Mulder, 1999; Harrell & Martin, 2015)), and many more are invalid owing to non-diagnostic holotype material. Previous researchers have made efforts to identify and remove invalid taxa, but the lack of a clear definition of the genus and type species has hindered this process.

Russell (1967) published one of the first diagnoses of the genus based on descriptive comparative study, but that diagnosis was based only on observations of North American *Mosasaurus* fossils, and Russell had not seen the holotype specimen. Therefore, While Russell's (1967) diagnosis adhered to the rules of

nomenclature, the data on which it was based were incomplete. Russell (1967) did, however, revise the taxonomy of *Mosasaurus* by sinking several junior synonyms and invalidating nine other species on the basis of insufficiently diagnostic type material, which resulted in eight valid species (*M. conodon*, *M. dekayi* Bronn, 1838, *M. gaudryi*, Dollo, 1889, *M. 'hoffmannii'*, *M. ivoensis*, Persson, 1963, *M. lonzeensis*, Dollo, 1904, *M. maximus* and *M. missouriensis*). Of these, *M. gaudryi* was reclassified as a tylosaurine (Bardet, 1990; Lindgren, 2005), and some confusion surrounds *M. lonzeensis* because Dollo (1904) named *M. lonzeensis* and *Hainosaurus lonzeensis* in the same article, differentiated the two, but did not provide a figure or specimen numbers for either so locating the original specimen of *M. lonzeensis* has proven difficult. Similarities between the enormous specimens of *M. maximus* from Maastrichtian deposits of North America and the generic type were recognized by Russell (1967), and *M. maximus* was synonymized with the type species, *M. hoffmannii*, by Mulder (1999). Lindgren & Siverson (2002) also reassigned Swedish *M. ivoensis* to *Tylosaurus*, and a species from southern England, *M. gracilis* Owen, 1849, was determined to be invalid and was reassigned to a group of non-mosasaurine mosasaurs (Street & Caldwell, 2014).

This study commenced by considering the species described by Russell (1967) and any species described since that publication as potentially valid. Russell (1967) did not address the Moroccan *Mosasaurus beaugei* Arambourg, 1952 and considered *M. lemonnieri* to be a junior synonym of *M. conodon*, but we will consider both in this discussion. We concur with the opinions of Mulder (1999) and Harrell & Martin (2015) that *M. maximus* is a junior synonym of *M. hoffmannii*, and with Lindgren & Siverson (2002) that *M. ivoensis* is a tylosaurine. These considerations result in ten species (*M. beaugei*, *M. conodon*, *M. dekayi*, *M. flemingi* Wiffen, 1990, *M. hobetsuensis*, Suzuki, 1985, *M. hoffmannii*, *M. lemonnieri*, *M. missouriensis*, *M. mokoroa*, and *M. prismaticus*, Sakurai, Chitoku & Shibuya, 1999) possibly belonging to *Mosasaurus*. Of these, only the type species and *M. missouriensis* have received much attention in recent years.

4.b. Status of species currently assigned to *Mosasaurus*

4.b.1. *Mosasaurus missouriensis* (Harlan, 1834)

M. missouriensis, known from upper Campanian strata from Kansas in the United States to Alberta in Canada, shares many similarities with *M. hoffmannii* and is the most completely known representative of the genus from North America. The quadrate differs from the type species in that the tympanic rim does not have a distinct anteroventral corner, nor is the oval stapedial pit oriented obliquely to the quadrate shaft. The tooth count for *M. missouriensis* is higher than for *M. hoffmannii* (maxilla = 15, dentary = 16, pterygoid = 9), and the carinae of the marginal teeth are consistent

along the length of the jaws. This species is now well defined and diagnosed (Konishi, Newbrey & Caldwell, 2014) and remains valid.

4.b.2. *Mosasaurus dekayi* Bronn, 1838

M. dekayi, known only from Maastrichtian strata from the East Coast of North America, is very poorly known. The various specimens assigned to the species comprise only laterally compressed, faceted, bicarinate teeth, isolated braincase elements and caudal vertebrae. Most likely, *M. dekayi* specimens represent posterior marginal dentition and smaller individuals of what would later be called *M. maximus*, and in future studies this material will be considered for reassignment to *M. hoffmannii*.

4.b.3. *Mosasaurus conodon* Cope, 1881

Cope (1881) only briefly and vaguely described the fragmentary specimen from the Maastrichtian greensands of New Jersey on which he based *M. conodon*. The imprecise definition has led to various and differing specimens from both Europe and North America being assigned to this species. There is very little overlap of complete elements between the holotypes of *M. conodon* and *M. hoffmannii*, but comparisons to more completely known taxa such as *M. missouriensis* confirms the classification of *M. conodon* as a mosasaurine. Differences between *M. conodon* and *M. hoffmannii* include a more gracile dentary bearing a greater number of teeth (likely > 16 in the former, 14 in the latter) that have smooth enamel and are not uniformly bicarinate. The short transverse processes of the cervical vertebrae are heavily buttressed ventrally in *M. conodon* as opposed to being elongate and relatively unbuttressed in the type species. Russell (1967) suggested that *M. lemonnieri* was a junior synonym of *M. conodon*, though this has since been refuted (Lingham-Soliar, 2000; Ikejiri & Lucas, 2015). The two species do share some morphological features, but there are specific differences that support retention of the two as separate species. Lingham-Soliar (2000) differentiated the two species based on features such as the ventral curvature of the dentary exhibited by *M. conodon* that is not seen in *M. lemonnieri*, and differing numbers of teeth in the dentary and pterygoid. Ikejiri & Lucas (2015) detailed numerous differences between the two taxa including a shorter, wider parietal table and a more elongate parietal foramen; a more robust posteroventral process of the jugal that is positioned more dorsally; and smooth, rather than faceted, tooth enamel in *M. conodon* in comparison to *M. lemonnieri*.

4.b.4. *Mosasaurus lemonnieri* Dollo, 1889

M. lemonnieri is one of the better-known species of *Mosasaurus* with multiple specimens collected from the Campanian – lower Maastrichtian phosphate quarries of Belgium. This species agrees largely with

M. hoffmannii but is generally smaller, more gracile and has higher tooth counts in all tooth-bearing elements (maxilla = 14–15, dentary = 16, pterygoid = 9–10). In these respects, *M. lemonnieri* is most similar to *M. missouriensis*. Like *M. hoffmannii*, the carinae on the marginal teeth are asymmetric anteriorly in *M. lemonnieri*, but the labial surface is fluted instead of faceted. Like *M. missouriensis* the quadrate of *M. lemonnieri* differs from the type species in lacking an anteroventral corner on the tympanic rim. The humerus of *M. lemonnieri* differs from *M. missouriensis* in being smoothly convex distally rather than bearing two distinct facets for the radius and ulna. This well-represented species appears to be valid.

4.b.5. *Mosasaurus beaugei* Arambourg, 1952

M. beaugei is known from Maastrichtian phosphatic deposits of Morocco (Arambourg, 1952; Bardet *et al.* 2004). Overall, its morphology agrees closely with *M. hoffmannii* but is distinguished at the species level by the low curvature of the anterior ramus of the jugal, the lack of a posteroventral process on the jugal and the greater anterior exposure of the splenial in lateral view. Additionally, while the marginal teeth are bicarinate and the carinae are asymmetrical anteriorly, the teeth are more compressed than in *M. hoffmannii*. The tooth count is maxilla = 12–13, dentary = 14–15, pterygoid = > 6. At this point in our analysis, we consider the species to be valid.

4.b.6. *Mosasaurus mokoroa* Welles & Gregg, 1971

M. mokoroa, from the Campanian of the South Island of New Zealand, exhibits the most differences in comparison to *M. hoffmannii*. Unlike *M. hoffmannii* the maxilla of *M. mokoroa* is significantly excavated dorsally for the external naris. Quadrate proportions are also different with the quadrate shaft being shorter ventral to the stapedial notch in *M. mokoroa* and the sub-circular stapedial pit not being oriented obliquely to the quadrate shaft. The marginal teeth of *M. mokoroa* are bicarinate, but the carinae are not asymmetrical anteriorly. The validity of this species is pending in-depth study of the assigned materials and comparisons to other Pacific Rim mosasaurids.

4.b.7. *Mosasaurus hobetsuensis* Suzuki, 1985

Found in upper Campanian to lower Maastrichtian deposits from Hokkaido, Japan, *M. hobetsuensis* also has very little material that overlaps with *M. hoffmannii*. The marginal teeth of *M. hobetsuensis* are bicarinate, unlike *M. conodon*, but are not as distinctly faceted as *M. hoffmannii* or even *M. missouriensis*. No cervical vertebrae of *M. hobetsuensis* are known, so no comparisons can be made to the holotype condition or the heavy buttressing of the transverse processes as seen in *M. conodon*. Paddle and pectoral girdle elements of *M. hobetsuensis* are generally similar to those of

M. conodon and *M. missouriensis*; however, the radius is more primitive and *Clidastes*-like. Like *M. mokoroa*, this species will be reviewed and its morphology compared to other Pacific Rim taxa in order to reassess the validity of this species.

4.b.8. *Mosasaurus flemingi* Wiffen, 1990

The one specimen of *M. flemingi* was found in Campanian–Maastrichtian-aged strata of the North Island of New Zealand. The holotype is comprised of posterior cranial elements, including a relatively complete left quadrate, and four articulated cervical vertebrae. The paroccipital bars are less robust than in *M. hoffmannii*, and the basisphenoid is less elongate with diverging basiptyergoid processes. The quadrate is not as tall ventral to the stapedial opening as the type species, and the tympanic rim lacks an anterodorsal corner. One of the most distinctive differences between *M. flemingi* and other species of *Mosasaurus* is the dorsoventral compression of the cervical centra. Like *M. mokoroa* and *M. hobetsuensis*, the validity and taxonomic assignment of this species will be assessed in a future study.

4.b.9. *Mosasaurus prismaticus* Sakurai, Chitoku & Shibuya, 1999

Another mosasaurine specimen, this one from upper Campanian strata, was discovered near Hobetsu on Hokkaido, Japan. The only overlap between this specimen and that of *M. hobetsuensis* is an isolated marginal tooth. However, while the teeth of *M. hobetsuensis* and *M. prismaticus* are compressed with well-developed carinae, that of *M. prismaticus* exhibits narrow facets or flutes, as opposed to the smooth enamel of *M. hobetsuensis*. Similar to *M. flemingi*, the holotype of *M. prismaticus* is comprised of posterior cranial elements. The anterior of the parietal preserves shallow depressions for the posterior prongs of the frontal, which generally agree with the *Mosasaurus* condition. However, the basiptyergoid processes of *M. prismaticus* are robust and divergent, giving the basisphenoid the more typical tetradiate morphology, rather than the anteriorly tapering form seen in *M. hoffmannii*. This species will also be assessed in more detail in a future study on Pacific mosasaurines.

4.c. Conclusions

It is not within the scope of this study to address the complete systematic revision necessary to prune the invalid species from *Mosasaurus*, but, using the emended diagnosis provided here, this will be a focus of future work. At this time, what is known is that *Mosasaurus* is a large mosasaurine that achieved cosmopolitan distribution from Campanian through to the end of Maastrichtian time. Most recent phylogenies (e.g. Dortangs *et al.* 2002) do not recover a monophyletic *Mosasaurus* clade, usually owing to the position of

Plotosaurus, with the phylogenetic relationships recovered by LeBlanc, Caldwell & Bardet (2012) being an exception.

The emended diagnoses of *Mosasaurus* and the type species *M. hoffmannii* provided above, which are, to date, the most comprehensive, strive to provide a more robust diagnosis for the genus. Within this framework it is possible to more accurately assess the validity of species that have been assigned to *Mosasaurus*. A forthcoming phylogenetic analysis will further serve to refine the sistergroup relationships of *M. hoffmannii* within *Mosasaurus* and with other members of the clade Mosasaurinae.

Acknowledgements. We thank N. Bardet, S. Chapman, A. Folie and A. Schulp for assistance during research visits to the collections they curate. Sincere thanks also to N. Bardet and T. Konishi for reviewing this lengthy manuscript and providing feedback that greatly improved the final version. An NSERC Discovery Grant 238458 and an NSERC Accelerator Grant, and a Faculty of Science, Chair's Research Allowance to MWC, supported this research. A Roger Soderstrom Scholarship granted to HPS by the Alberta Historical Resources Foundation and funded by the Alberta Lotto additionally supported this research.

References

- ARAMBOURG, C. 1952. Les vertébrés fossiles des gisements de phosphates (Maroc – Algérie – Tunisie). *Notes et Mémoires du Service Géologique du Maroc* **92**, 1–372.
- BARDET, N. 1990. Première mention du genre *Hainosaurus* (Squamata, Mosasauridae) en France. *Comptes Rendus de l'Académie des Sciences, Série II* **311**, 751–6.
- BARDET, N. 2012a. The mosasaur collections of the Muséum National d'Histoire Naturelle of Paris. *Bulletin de la Société géologique de France* **183**, 35–53.
- BARDET, N. 2012b. Maastrichtian marine reptiles of the Mediterranean Tethys: a palaeobiogeographical approach. *Bulletin de la Société géologique de France* **183**, 573–96.
- BARDET, N., FALCONNET, J., FISCHER, V., HOUSSAYE, A., JOUVE, S., PEREDA SUBERBIOLA, X., PÉREZ-GARCÍA, A., RAGE, J.-C. & VINCENT, P. 2014. Mesozoic marine reptile palaeobiogeography in response to drifting plates. *Gondwana Research* **26**, 869–87.
- BARDET, N. & JAGT, W. M. 1996. *Mosasaurus hoffmannii*, le “Grand animal fossile des carrières de Maestricht”: deux siècles d'histoire. *Bulletin du Muséum National d'Histoire Naturelle Paris 4^e série*, **18, Section C n°4**, 569–93.
- BARDET, N., PEREDA SUBERBIOLA, X., LAROCHE, M., BOUYAHYAOU, F., BOUYA, B. & AMAGHZAZ, M. 2004. *Mosasaurus beaugei* Arambourg, 1952 (Squamata, Mosasauridae) from the Late Cretaceous phosphates of Morocco. *Geobios* **37**, 315–24.
- BELL, G. L. JR. 1997. A phylogenetic revision of North American and Adriatic Mosasauridae. In *Ancient Marine Reptiles* (eds J. M. Callaway & E. L. Nicholls), pp. 293–332. San Diego: Academic Press.
- BRONN, H. G. 1838. *Lethaea Geognostica*. Erster Band. Stuttgart: E. Schweizerbart's Verlagshandlung, 768 pp.
- BUC'HOZ, P. J. 1782. *Les dons Merveilleux et Diversément Coloriés de la Nature dans le Règne Minéral, ou Collection de Minéraux Précieusement Coloriés, pour Servir à l'Intelligence de l'Histoire Naturelle et Oeconomique des Trois Règnes*. Paris: Chez l'auteur, 100 pp.
- CALDWELL, M. W. & PALCI, A. 2007. A new basal mosasaurid from the Cenomanian (U. Cretaceous) of Slovenia with a review of mosasaurid phylogeny and evolution. *Journal of Vertebrate Paleontology* **27**, 863–80.
- CAMP, C. L. 1942. *California Mosasaurs*. Berkeley, Los Angeles: University of California Press, 51 pp.
- CAMPER, P. 1786. Conjectures relative to the petrifications found in St. Peter's Mountain, near Maestricht. *Philosophical Transactions of the Royal Society of London B* **76**, 443–56.
- CAMPER, A. G. 1800. Sur les ossements fossiles de la montagne de St. Pierre, à Maëstricht. *Journal de Physique, de Chimie et d'Histoire Naturelle* **51**, 278–91.
- CAMPER, A. G. 1812. Mémoires sur quelques parites moins connues du squelette des sauriens fossiles de Maestricht. *Annales du Muséum d'Histoire Naturelle* **19**, 215–41.
- CHARLESWORTH, E. 1846. On the occurrence of the *Mosasaurus* in the Essex Chalk, and on the discovery of flint within the pulp-cavities of its teeth. *British Association for the Advancement of Sciences* **1845**, 60.
- CONYBEARE, W. D. 1822. *Mosasaurus*.—The saurus of the Meuse, the Maestricht animal of Cuvier. In *An Introduction to the Study of Fossil Organic Remains* (ed. J. Parkinson), pp. 298. London: Sherwood, Neely and Jones, and W. Phillips.
- COPE, E. D. 1868. Remarks on *Clidastes iguanavus*, *Nectoporphus validus*, and *Elasmosaurus*. *Proceedings of the Academy of Natural Sciences* **20**, 181.
- COPE, E. D. 1869. On the reptilian orders Pythonomorpha and Streptosauria. *Proceedings of the Society of Natural History* **12**, 250–66.
- COPE, E. D. 1870. Synopsis of the extinct Batrachia, Reptilia, and Aves of North America. *Transactions of the American Philosophical Society* **Part 2**, 106–235.
- COPE, E. D. 1881. A new species of *Clidastes* from New Jersey. *American Naturalist* **15**, 587–8.
- CUVIER, G. 1808. Sur le grand animal fossile des carrières de Maestricht. *Annales du Muséum d'Histoire Naturelle* **12**, 145–76.
- CUVIER, G. 1829. *Le Règne Animal Distribué d'après son Organization, pour Servir de Base à l'Histoire Naturelle des Animaux et d'Introduction à l'Anatomie Comparée*. Volume 2. 2nd edition. Paris: Déterville Libraire, 406 pp.
- DOLLO, L. 1882. Note sur l'ostéologie des Mosasauridae. *Bulletin du Muséum d'histoire Naturelle de Belgique* **1**, 55–80.
- DOLLO, L. 1889. Première note sur les mosasours de Mesvin. *Bulletin de la Société belge de Géologie, de Paléontologie et d'Hydrologie* **3**, 271–304.
- DOLLO, L. 1904. Les mosasauriens de la Belgique. *Bulletin de la Société belge de Géologie, de Paléontologie et d'Hydrologie* **18**, 207–16.
- DOLLO, L. 1924. *Globidens alabamaensis*, mosasaurien américain retrouvé dans le Craie d'Obourg (Sénonien supérieur) du Hainaut, et les mosasours de la Belgique en general. *Archives de Biologie* **34**, 167–213.
- DORTANGS, R. W., SCHULP, A. S., MULDER, E. W. A., JAGT, J. W. M., PEETERS, H. H. G. & DE GRAAF, D. T. 2002. A large new mosasaur from the Upper Cretaceous of The Netherlands. *Netherlands Journal of Geosciences* **81**, 1–8.
- FAUJAS DE SAINT-FOND, B. 1799. *Histoire Naturelle de la Montagne de Saint-Pierre de Maëstricht*. Paris: J. Jansen, 263 pp.

- GERVAIS, P. 1848–1852. *Zoologie et Paléontologie Françaises (Animaux Vertébrés), ou Nouvelles Recherches sur les Animaux Vivants et Fossiles de la France*. First edition. Paris: Libraire Arthus Bertrand, 271 pp.
- HARLAN, R. 1834. Notice of the discovery of the remains of the *Ichthyosaurus* in Missouri, N. A. *Transactions of the American Philosophical Society, New Series* **4**, 405–8.
- HARLAN, R. 1839a. Notice of the discovery of *Basilosaurus* and *Batrachiosaurus*. *Proceedings of the Geological Society of London* **3**, 23–4.
- HARLAN, R. 1839b. Letter regarding *Basilosaurus* and *Batrachiotherium*. *Bulletin de la Société géologique de France 1^o serie* **10**, 89–90.
- HARRELL, T. L. & MARTIN, J. E. 2015. A mosasaur from the Maastrichtian Fox Hills formation of the northern Western Interior Seaway of the United States and the synonymy of *Mosasaurus maximus* with *Mosasaurus hoffmanni* (Reptilia: Mosasauridae). *Netherlands Journal of Geosciences* **94**, 23–37.
- HOLL, F. 1829. *Handbuch der Petrefactenkunde*. Dresden: P. G. Hilschersche Buchhandlung 232 pp.
- IKEJIRI, T. & LUCAS, S. G. 2015. Osteology and taxonomy of *Mosasaurus conodon* Cope 1881 from the Late Cretaceous of North America. *Netherlands Journal of Geosciences* **94**, 39–54.
- KONISHI, T., BRINKMAN, D., MASSARE, J. A. & CALDWELL, M. W. 2011. New exceptional specimens of *Prognathodon overtoni* (Squamata, Mosasauridae) from the upper Campanian of Alberta, Canada, and the systematics and ecology of the genus. *Journal of Vertebrate Paleontology* **31**, 1026–46.
- KONISHI, T. & CALDWELL, M. W. 2011. Two new pliolatecarpine (Squamata, Mosasauridae) genera from the Upper Cretaceous of North America, and a global phylogenetic analysis of pliolatecarpines. *Journal of Vertebrate Paleontology* **31**, 754–83.
- KONISHI, T., NEWBREY, M. & CALDWELL, M. W. 2014. A small, exquisitely preserved specimen of *Mosasaurus missouriensis* (Squamata: Mosasauridae) from the upper Campanian of the Bearpaw Formation, western Canada and the first stomach contents for the genus. *Journal of Vertebrate Paleontology* **34**, 802–19.
- KUYPERS, M. M. M., JAGT, J. W. M., PEETERS, H. H. G., DE GRAAF, D. T., DORTANGS, R. W., DECKERS, M. J. M., EYSERMANS, D., JANSSEN, M. J. & ARPOT, L. 1998. Laat-kretaceïsche mosasauriers uit Luik-Limburg: nieuwe vondsten leiden tot nieuwe inzichten. *Publicaties van het Natuurhistorisch Gentschap in Limburg* **41**, 5–47.
- LEBLANC, A. R. H., CALDWELL, M. W. & BARDET, N. 2012. A new mosasaurine from the Maastrichtian (Upper Cretaceous) Phosphates of Morocco and its implications for mosasaurine systematics. *Journal of Vertebrate Paleontology* **32**, 82–104.
- LEBLANC, A. R. H., CALDWELL, M. W. & LINDGREN, J. 2013. Aquatic adaptation, cranial kinesis, and the skull of the mosasaurine mosasaur *Plotosaurus bennisoni*. *Journal of Vertebrate Paleontology* **33**, 349–62.
- LEIDY, J. 1856. Notices of the extinct vertebrated animals discovered by Prof. E. Emmons. *Proceedings of the Academy of Natural Sciences* **8**, 255–6.
- LEIDY, J. 1861. Remarks on remains of some extinct Vertebrata in the territory of Nebraska. *Proceedings of the American Philosophical Society* **7**, 10–11.
- LEIDY, J. 1865. Memoir of the extinct reptiles of the Cretaceous formations of the United States. *Smithsonian Contributions to Knowledge* **14**(6), 1–165.
- LINDGREN, J. 2005. The first record of *Hainosaurus* (Reptilia: Mosasauridae) from Sweden. *Journal of Paleontology* **76**, 1157–65.
- LINDGREN, J. & SIVERSON, M. 2002. *Tylosaurus ivoensis*: a giant mosasaur from the early Campanian of Sweden. *Earth and Environmental Science Transactions of the Royal Society of Edinburgh* **93**, 73–93.
- LINGHAM-SOLIAR, T. 1991. Mosasaurs from the Upper Cretaceous of the Republic of Niger. *Palaeontology* **34**, 653–70.
- LINGHAM-SOLIAR, T. 1995. Anatomy and functional morphology of the largest marine reptile known, *Mosasaurus hoffmanni* (Mosasauridae, Reptilia) from the Upper Cretaceous, Upper Maastrichtian of the Netherlands. *Philosophical Transactions of the Royal Society of London B* **347**, 155–72.
- LINGHAM-SOLIAR, T. 2000. The mosasaur *Mosasaurus lemmonieri* (Lepidosauromorpha, Squamata) from the Upper Cretaceous of Belgium and The Netherlands. *Paleontological Journal* **34**(Suppl.), S225–37.
- LINGHAM-SOLIAR, T. & NOLF, D. 1989. The mosasaur *Prognathodon* from the Upper Cretaceous of Belgium (Reptilia, Mosasauridae). *Bulletin de l'Institut Royal des Sciences Naturelles de Belgique* **59**, 137–90.
- LINNAEUS, C. 1758. *Systema Naturae, Secundum Classes, Ordines, Genera, Species, cum Characteribus, Differentiis, Synonymis, Locis. Tomus I. Editio Decima, Reformata*. Stockholm: Laurentii Salvii, 824 pp.
- MANTELL, G. A. 1829. A tabular arrangement of the organic remains of the county of Sussex. *Transactions of the Geological Society, Second Series* **3**, 201–16.
- MEIJER, A. W. F. 1983. Der vondst van een onderkaaksbeen van een onbekende Mosasauriër (Reptilia, Mosasauridae) in de Sibbergroeve. *Natuurhistorisch Maandblad Maastricht* **72**, 269–71.
- MEYER, H. VON. 1832. *Palaeologica zur Geschichte der Erde und ihrer Geschöpfe*. Frankfurt: S. Schmerber, 560 pp.
- MULDER, E. W. A. 1999. Transatlantic latest Cretaceous mosasaurs (Reptilia, Lacertilia) from the Maastrichtian type area and New Jersey. *Geologie en Mijnbouw* **78**, 281–300.
- OPPEL, M. 1811. *Die Ordnungen, Familien, und Gattungen der Reptilien als Prodrum Einer Naturgeschichte Derselben*. Munich: Joseph Lindauer, 86 pp.
- OWEN, R. 1840–1845. *Odontography*. London: H. Baillière, 762 pp.
- OWEN, R. 1849. *A History of British Fossil Reptiles Volume 1*. London: Cassel and Company Limited, 667 pp.
- PARKINSON, J. 1822. *Outlines of Oryctology: An Introduction to the Study of Fossil Organic Remains; Especially of Those Found in the British Strata: Intended to Aid the Student in His Inquiries Respecting the Nature of Fossils and Their Connection with the Formation of the Earth*. London: Sherwood, Neely and Jones, and W. Phillips, 346 pp.
- PERSSON, P. O. 1959. Reptiles from the Senonian of Scania. *Arkiv for Kemi Mineralogi och Geologi* **2**, 431–80.
- PERSSON, P. O. 1963. Studies on Mesozoic marine reptile faunas with particular regard to the Plesiosauria. *Publications from the Institutes of Mineralogy, Paleontology, and Quaternary Geology, University of Lund, Sweden* **118**, 1–15.
- PIETERS, F. J. M., ROMPEN, P. G. W., JAGT, J. W. M. & BARDET, N. 2012. A new look at Faujas de Saint-Fond's fantastic story on the provenance and acquisition of the type specimen of *Mosasaurus hoffmanni* Mantell, 1829. *Bulletin de la Société Nationale de Géologie de France* **183**, 55–65.

- RUSSELL, D. A. 1967. Systematics and morphology of American mosasaurs. *Bulletin of the Peabody Museum of Natural History* **23**, 241 pp.
- SAKURAI, K., CHITOKU, T. & SHIBUYA, N. 1999. A new species of *Mosasaurus* (Reptilia, Mosasauridae) from Hobetsu, Hokkaido, Japan. *Bulletin of the Hobetsu Museum* **15**, 53–66.
- SÖMMERING, S. T. VON. 1816. Ueber die *Lacerta gigantean* der Vorwelt. *Denkschriften der Königlichen Akademie der Wissenschaften zu Münch* **6**, 37–59.
- STREET, H. P. & CALDWELL, M. W. 2014. Reassignment of Turonian mosasaur material from the ‘Middle Chalk’ (England, U.K.), and the status of *Mosasaurus gracilis* Owen, 1849. *Journal of Vertebrate Paleontology* **34**, 1072–9.
- SUZUKI, S. 1985. A new species of *Mosasaurus* (Reptilia, Squamata) from the Upper Cretaceous Hakobuchi Group in Central Hokkaido, Japan. In *Evolution and Adaptation of Marine Vertebrates* (eds M. Goto, M. Takahashi, M. Kimura & H. Horikawa), pp 45–66. Association for Geological Collaboration in Japan, Monograph no. 30.
- UBAGHS, C. 1879. Description de quelques grand vertébrés de la Craie Supérieure de Maastricht. *Description Géologique et Paléontologique du sol du Limbourg* **1879**, 238–49.
- VAN MARUM, M. 1790. Beschryving der beenderen van den kop van eenen visch, gevonden in den St. Pietersberg by Maastricht, en geplaatst in Teylers Museum. *Verhandelingen van Teylers Tweede Genootschap* **8**, 383–9.
- WELLES, S. P. & GREGG, D. R. 1971. Late Cretaceous marine reptiles of New Zealand. *Records of the Canterbury Museum* **9**, 1–111.
- WIFFEN, J. 1990. New mosasaurs (Reptilia; Family Mosasauridae) from the Upper Cretaceous of North Island, New Zealand. *New Zealand Journal of Geology and Geophysics* **33**, 67–85.
- YOUNG, M. T. & DE ANDRADE, M. B. 2009. What is *Geosaurus*? Redescription of *Geosaurus giganteus* (Thalattosuchia: Metriorhynchidae) from the Upper Jurassic of Bayern, Germany. *Zoological Journal of the Linnean Society* **157**, 551–85.